Visual pigments, ocular filters and the evolution of snake vision

Bruno F. Simões[1,*], Filipa L. Sampaio[1], Ronald H. Douglas[2], Ullasa Kodandaramaiah[3], Nicholas R. Casewell[4], Robert A. Harrison[4], Nathan S. Hart[5], Julian C. Partridge[6], David M. Hunt[6,7] & David J. Gower[1,*].

[1]Department of Life Sciences, The Natural History Museum, London, SW7 5BD, UK; [2]Department of Optometry and Visual Science, City University London, London EC1V 0HB, UK; [3]School of Biology, Indian Institute of Science Education and Research Thiruvananthapuram, Thiruvananthapuram 695 016, India; [4]Alistair Reid Venom Research Unit, Liverpool School of Tropical Medicine, Pembroke Place, Liverpool L3 5QA, UK; [5]Department of Biological Sciences, Macquarie University, North Ryde, NSW 2109, Australia; [6]School of Animal Biology and The Oceans Institute, The University of Western Australia, Perth, WA 6009, Australia; [7]Lions Eye Institute, University of Western Australia, Perth, 6009, Australia

*Email: bruno.simoes@me.com; d.gower@nhm.ac.uk

Abstract

Much of what is known about the molecular evolution of vertebrate vision comes from studies of mammals, birds and fish. Reptiles (especially snakes) have barely been sampled in previous studies despite their exceptional diversity of retinal photoreceptor complements. Here we analyse opsin gene sequences and ocular media transmission for up to 69 species to investigate snake visual evolution. Most snakes express three visual opsin genes (*rh1, sws1, lws*). These opsin genes (especially *rh1* and *sws1*) have undergone much evolutionary change, including modifications of amino acid residues at sites of known importance for spectral tuning, with several tuning site combinations unknown elsewhere among vertebrates. These changes are particularly common among dipsadine and colubrine 'higher' snakes. All three opsin genes are under purifying selection, though dN/dS varies with respect to some lineages, ecologies, and retinal anatomy. Positive selection was detected at multiple sites in all three opsins, these being concentrated in transmembrane domains and thus likely to have a substantial effect on spectral tuning and other aspects of opsin function. Snake lenses vary substantially in their spectral transmission. Snakes active at night and some of those active by day have very transmissive lenses, while some primarily diurnal species cut out shorter wavelengths (including UVA). In terms of retinal anatomy, lens transmission,

visual pigment spectral tuning and opsin gene evolution the visual system of snakes is more diverse than in any other tetrapod order.

Key words: ocular media, sensory evolution, photoreception, Serpentes, spectral tuning, vision

Introduction

Animal vision has become one of the best examples of the power of integrative biology. A great deal is known about the anatomy of eyes at many levels, but much is also known about how eyes function and have evolved, including aspects of the physiology underlying photon capture, spectral sensitivity, signal transduction and propagation, and the identity of several key genes and proteins. Indeed, vision is one of the best characterized of all biological sensory systems. In addition, selective pressures can often be determined from physical first principles, allowing the identification and quantification of many aspects of the evolution of eyes (Land 1981; Nilsson 1996). In general, vision in vertebrates is especially well studied, and studies of the evolution of their visual pigments have been able to both identify evolutionary changes, and to ascribe such changes to adaptive evolutionary processes (e.g. Hughes 2008).

The fundamentals of vertebrate vision have been particularly well studied in terms of the molecular basis of photoreception and phototransduction. A cornerstone of this is knowledge of the photosensitivity of visual pigments, members of the large family of G-protein-coupled-receptor (GPCR) proteins, which share a common arrangement of an opsin protein linked to a chromophore derived from vitamin A (Wald 1968). Visual pigments play a core role in photon detection and colour vision and they are a leading example of how gene duplications (Dulai et al. 1999) and changes in amino acid sequences (Yokoyama 2008), type of chromophore (vitamin A1 or A2: Enright et al. 2015) and gene expression (Hofmann and Carleton 2009; Carleton et al. 2010) underlie adaptations to differing ecological and behavioural selection pressures. Visual opsins in some vertebrates have been intensely studied over the past 20 years, to the extent that changes in specific amino acid ('spectral tuning') sites are known to change the peak absorbance wavelength (λ_{max}) of the visual pigments (Yokoyama 2008; Yokoyama et al. 2014). However, there is no universal consensus about the tuning impacts of all such mutations (Hauser et al. 2014), with some data suggesting that additional mechanisms to change spectral sensitivity may exist (Davies et al. 2009; Martin et al. 2015).

Much of our knowledge about the function and evolution of vertebrate vision, including its molecular basis, comes from empirical studies on a relatively small proportion of living vertebrates, predominantly some groups of mammals, birds and fish (Nickle and Robinson 2007; Davies et al. 2012). Investigation of vision in other

vertebrates is needed to test inferred generalities, especially in those taxa having visual systems with very different anatomical arrangements of the eye, and/or great phenotypic diversity. Snakes are one such lineage that shows substantial diversity of ocular anatomy, especially retinal photoreceptor complement. Indeed, Walls (1942) and Underwood (1967; 1970) argued that, by virtue of their great diversity of photoreceptor complements, there must have been more evolutionary changes within snakes than in all the other vertebrates combined. The eyes of snakes are also remarkable for being highly divergent in gross morphology from that of non-snake squamates ('lizards'), in lacking photoreceptor oil droplets, in mostly being covered by a transparent head scale (spectacle or Brille), and in presenting evidence for evolutionary transitions ('transmutation' sensu Walls 1934) between rods and cones (Walls 1942).

The approximately 3,500 species of living snakes are distributed across all continents except Antarctica (Van Wallach et al. 2014). They are very diverse ecologically (e.g., Greene 1997) and include burrowing, arboreal, gliding, fully aquatic, nocturnal and diurnal species. Some have small eyes lying under typical head scales, while others are visual hunters with well developed binocular vision, some of which have horizontal pupils and a fovea (Walls 1942). Since Walls' and Underwood's pioneering anatomical surveys, we have learned that the ancestral snake likely had three of the five visual opsin genes present in the ancestral vertebrate (Davies et al. 2009; Simões et al. 2015), but not much more is known.

In order for light to be absorbed by the visual pigments it first has to pass through the ocular media. In vertebrates these comprise the cornea, lens, and aqueous and vitreous humour. Snakes additionally have a covering over the cornea (brille or spectacle). Lens transmission characteristics of most major vertebrate groups have been widely studied (e.g. Douglas and Marshall 1999; Douglas and Jeffery 2014 for reviews), but there are few reports of the spectral transmission of snake lenses. Walls (1931) noted yellow (blue-absorbing) lenses in a number of diurnal snakes and uncoloured lenses in nocturnal species. However, these observations were qualitative, using the UV-insensitive human visual system, such that the spectral characteristics of both coloured and transparent lenses in the UV are unknown, with the exception of two species of sea snake whose lenses transmit significant amounts of UV (Hart et al. 2012). The spectral characteristics of the reptilian spectacle have been reported only twice (Hart et al. 2012; van Doorn and Sivak 2015).

Given the anatomical diversity of snake retinal photoreceptors and the relative lack of previous studies, we address the following major questions: (1) What are the major patterns in the diversity and molecular evolution of snake visual opsins? (2) Is the diversity in retinal photoreceptor anatomy, visual opsin and ocular media transmission

linked in a predictable way? (3) To what extent is visual opsin spectral tuning and/or opsin molecular evolution explained by major shifts in ecology and/or retinal anatomy? (4) Do snakes present diversity in visual opsins beyond that known for other major groups of vertebrates, mirroring the diversity of their ocular morphology?

Here we report the largest dataset of visual opsin genes in reptiles to date, covering the major types of snake retinal anatomy and taxonomic and ecological diversity. We also report data on the spectral transmission of important components of the ocular media (lens and spectacle) of a subset of these snakes. We find that although the vast majority of snakes retain three of the visual opsin genes likely present in the ancestral snake, these have undergone considerable diversification through functionally important amino acid substitutions. Notably, many of these substitutions are unreported in other vertebrate groups. There are also changes in the transmission of the lens, particularly with respect to the filtering of short wavelengths that will significantly affect overall spectral sensitivities. Snakes are an important system for understanding of the evolution of the vertebrate visual system.

Material & Methods

Taxon sampling and sample storage

Snakes were acquired through fieldwork, the Liverpool school of Tropical Medicine, from hobbyists and the commercial trade. Our sampling (SI Table S1) aimed to maximise taxonomic (phylogenetic), ecological and ocular anatomical diversity. One specimen each of 48 species was newly sampled. The use of animals in this research was conducted using standard protocols approved by the Liverpool school of Tropical Medicine Animal Welfare and Ethical Review Board and the UK Home Office. Following euthanasia, spectacle scales (brilles) were removed and the eyes extracted. After removing the lens, each eye was coarsely macerated and stored in RNAlater (Ambion) at -80°C until the RNA extraction. Where possible, undamaged lenses and spectacles were stored dry at -20°C until measurement of spectral transmission was performed.

RNA extraction and cDNA synthesis

Total RNA was extracted from eyes using TRIzol® (Life Technologies/Ambion) followed by purification with PureLink™ RNA Mini Kit (Life Technologies/Ambion) using the manufacturer's protocol. First-strand complementary DNA (cDNA) was synthesized with a Transcriptor First Strand cDNA Synthesis Kit (Roche) with 500ng of total RNA according to manufacturer's instructions. RNA complementary to the cDNA was removed using 2

146 units of *E. coli* RNase H (Ambion) and incubated at 37°C for 20 minutes. For the
147 following species freshly synthesized cDNA was dehydrated, stored at ambient
148 temperature for 24 hours, and returned to -20°C and rehydrated after a further 24
149 hours before subsequent amplification: *Melanophidium* sp., *Uropeltis* cf. *macrolepis*,
150 *Gongylophis conicus, Pareas monticola, Amphiesma stolata, Xenochrophis piscator,*
151 *Xylophis captaini, Boiga forsteni, Boiga ceylonensis.* All other cDNA samples were kept
152 hydrated and stored at -20°C prior to amplification.

153

154 *Visual opsin gene amplification and cloning*

155 Here we denote opsin genes in lower case italics and opsin proteins in upper case (e.g.
156 *rh1* and RH1, respectively). We amplified the coding regions of *sws1, lws* and *rh1* visual
157 opsin genes using universal primers designed to amplify visual opsin genes across snakes
158 and squamates (Simões et al. 2015). All fragments were amplified in 25 µl Polymerase
159 Chain Reactions (PCR): 1x PCR buffer (Invitrogen), 1.5 mmol (mM) of $MgCl_2$ (Invitrogen),
160 50 µmol/L of deoxynucleotides (Bioline), 0.4 µmol/L of each primer and 1 unit Platinum
161 Taq Polymerase (Invitrogen) and 100ng of cDNA. PCR products were amplified by
162 touchdown PCR with the following cycling parameters: initial denaturation at 95°C for 5
163 minutes; 20 cycles of 1 minute at 95°C (denaturation), 30 seconds at 60°C (annealing),
164 and 1 minute at 72°C (extension) with a decrease of 0.5°C per cycle; 15 cycles of 1
165 minute at 95°C (denaturation), 30 seconds at 50°C (annealing), and 1 minute at 72°C
166 (extension) followed by a final extension at 72°C for 5 minutes. PCR products were run
167 on a 1% agarose gel, excised in a Blue Light Transilluminator (Safe Imager, Invitrogen)
168 and purified with a PureLink Quick Gel Extraction Kit (Invitrogen). PCR fragments were
169 cloned with a StrataClone PCR Cloning Kit (Agilent) and corresponding chemically
170 competent cells following the manufacturer's protocol. Transformed cells were grown
171 overnight on agar medium treated with 100 mg/ml of Ampicilin (Bioline) and 1ml of 2%
172 X-GAL at 37°C. Sixteen white colonies were picked and used as DNA template in 25µl
173 PCR reactions: 1x PCR buffer (Bioline), 1 mmol (mM) of $MgCl_2$ (Bioline), 80 µmol/L of
174 deoxynucleotides (Bioline), 0.2 µmol/L of M13F and M13R vector primers and 1 unit of
175 BioTAQ Polymerase (Bioline) and 2µl of DNA (1 colony twirled in 50µl of ultra-pure
176 water). The PCR had the following cycling parameters: initial denaturation at 95°C for 10
177 minutes; 30 cycles of 15 seconds at 95°C (denaturation), 30 seconds at 58°C (annealing),
178 and 1 minute and 30 seconds at 72°C (extension) and a final extension at 72°C for 1.5
179 minutes. Between four and eight positive clones were sequenced in both directions with
180 M13 universal primers in an automated DNA sequencer. Sequences were assembled in
181 Geneious R8 (Kearse et al. 2012) and are deposited in GenBank, accession numbers
182 XXXX-XXXX (SI Table S1).

Barcoding

Genomic DNA (gDNA) was extracted from each eye tissue sample using the DNA layer in Trizol of the RNA extraction, following the Trizol manufacturer's instructions and/or from muscle tissue stored in ethanol using the Qiagen blood and tissue kit. We generated mitochondrial *16s rRNA* 'barcodes' for most specimens (SI Table S1) using universal primers (Palumbi, 1996) in 25 µl PCR reactions: 1x PCR buffer (Invitrogen), 1 mmol (mM) of $MgCl_2$ (Invitrogen), 50 µmol/L of deoxynucleotides (Bioline), 0.4 µmol/L of each primer and 1 unit Platinum Taq Polymerase (Invitrogen) and 100ng of gDNA. The PCR cycling parameters were: initial denaturation at 95°C for 10 minutes; 30 cycles of 15 seconds at 95°C (denaturation), 30 seconds at 55°C (annealing), and 1 minute at 72°C (extension) and a final extension at 72°C for 1 minute. All successfully amplified products were sequenced in both directions using the same primers used for PCR, in an automated DNA sequencer. The barcodes were assembled in Geneious R8.

Phylogenetic analysis

Visual opsin gene cDNA sequences were aligned with published sequences from other reptiles including other snakes (SI, Table S1) with MAFFT (Katoh et al. 2002) (settings: algorithm; auto; gap penalty: 3; off-set value: 0.1) implemented in Geneious R8, Muscle (Edgar, 2004) (default settings: 15 interactions), and PRANK (Löytynoja and Goldman, 2005) (HKY model with empirical base frequencies and kappa=2). These alignments were inspected by eye for both nucleotides and amino acids and were adjusted manually to ensure nucleotides were in-frame and that indels did not include partial codons. The final alignments based on the results of all three programs were identical. jModelTest 2 (Darriba et al. 2012) was used to ascertain the best-fit model of sequence evolution for each alignment according to their AIC and BIC scores. GTR+G+I was the best-fitting model for the three visual opsin genes amplified. Given concerns about incorrectly estimating G when including I in the model (Yang, 2006), we also ran analyses under GTR+G. Phylogenetic analyses were conducted using Maximum (ML) Likelihood and Bayesian Inference (BI) approaches. ML analyses were run with RAxML v8 (Stamatakis 2014) using majority rule bootstopping criteria (Pattengale et al. 2009); randomized MP starting trees, and a fast hill-climbing algorithm. BI analyses were run with Mr. Bayes v3.1.2 (Huelsenbeck and Ronquist 2001) for 1,000,000 generations with chains sampled every 100 generations (after 25% of trees were discarded as burn-in), random starting trees, 4 chains (3 hot and 1 cold), and convergence was assumed when the standard deviation of split frequencies fell below 0.01. Gekkota was used as the

outgroup to root the *sws1* and *lws* trees, and other non-snake squamate visual opsin gene sequences were used to root the *rh1* tree (SI Table S1).

Analyses of molecular evolution

We used selection test analyses to identify patterns in visual opsin gene evolution across the snake evolutionary tree (using branch models) and within the individual visual opsin genes (site models). Codeml implemented in the PAML 4.7 package (Yang 2007) was used to estimate non-synonymous (dN) and synonymous (dS) substitution rates and the respective ratio (dN/dS, or ω) for the *sws1, lws* and *rh1* genes in snakes. Sequence alignment indels were removed if present in only one taxon or recoded as missing data if present in more.

Branch models (Yang 1998) allow the ω ratio to vary across branches in the tree and can be used to infer positive selection (ω>1) acting in particular lineages. The simplest branch model (one-ratio) allows only one ω ratio value across the tree, whereas the more complex free-ratio model assumes independent ω ratios for each branch. Branch models were also used to estimate ω for two branch categories based on ecotypes (primarily fossorial or not, aquatic/semiaquatic or not, primarily arboreal or not, primarily diurnal or not). The ecological classification applied to each species is reported in Fig. 1 and Table S2. Given the substantial diversity of retinal morphology, ecology and density of our sampling within the family, we also estimated two-ratio branches within Colubridae alone. All branch models were compared using the Likelihood Ratio Test (LRT) and the simpler model (one-ratio) was rejected where $p<0.05$. Branch models were also carried out for a subset of taxa for which the photoreceptor cell complement is known (SI Table S2) to test for possible links between molecular evolution and the presence/absence of double cones or transmuted (sensu Walls 1934) rod-like cones. Retinal anatomy is not known for all species sampled so we removed such taxa from the data set for corresponding molecular evolution analyses and pruned them from the phylogeny in investigations of the relationship between opsin gene evolution and retinal morphology.

Site models (M1a nearly-neutral and M2a positive selection; M7β and M8 β&ω) allow ω to vary among sites (amino-acids or codons) (Yang et al. 2000). Site models M2a and M8 were compared (using LRT) with the simpler site models M1a and M7, respectively and the simpler models rejected where $P>0.05$. Bayes empirical Bayes (BEB) (Yang et al. 2005) implemented in models M2a and M8 β&ω was used to identify sites inferred to be under positive selection for each visual opsin gene.

Under branch-site models, ω can vary across both sites and lineages (Zhang 2005) and this was used to infer positive selection at sites among major lineages of snakes (Colubridae, snakes with transmuted, rod-like cones and snakes that are primarily fossorial, arboreal, aquatic/semiaquatic and diurnal). Branch-site models were compared with the simplest model M1a using LRT. Ancestral visual opsin gene sequences were estimated by marginal and joint reconstruction using Codeml.

We used PRIME analysis executed on the Datamonkey server (Delport et al. 2010) to estimate amino acid exchangeability (as in BEB) but also radical substitutions that result in amino acids with very different biochemical properties. We used both sets of five amino-acid properties available in PRIME: Conant-Stadler (Conant et al. 2007) and Atchley et al. (Atchley et al. 2005). CMS (Delport et al. 2010) was used to identify the most appropriate codon model for PRIME analysis.

For analyses of molecular evolution and ancestral state reconstruction we used a phylogenetic tree congruent with those published by (Wiens et al. 2012; Pyron et al. 2013; Reeder et al. 2015) (Species Tree, Figure 1). Although the monophyly of the colubrid clades Colubrinae, Natricinae and Dipsadinae are well supported (e.g., Wiens et al. 2012; Pyron et al. 2013), there is currently no compelling resolution of the relationships among them. Thus, as well as following the weakly supported resolution in the trees of (Pyron et al. 2013) (Colubrinae lying outside Natricinae+Dipsadinae), we accounted for phylogenetic uncertainty and repeated the branch and site model analyses for the two alternative phylogenetic resolutions: ((Dipsidinae, Colubrinae), Natricinae) and ((Natricinae, Colubrinae), Dipsidinae). The Indian snake *Xylophis captaini* or any congeners have not yet been included in molecular phylogenetic analyses. Although some workers have reported similarities between *Xylophis* and xenodermatids (e.g,. McDowell 1987), we consider the similarity to the Sri Lankan *Aspidura* suggestive of phylogenetic affinity (e.g., Gans and Fetcho 1982; Gower and Winkler 2007) and so we include it as a correspondingly resolved natricine here.

Chi-squared tests of null hypotheses that sites inferred to be under positive selection do not occur unevenly among functional bipartitions (trans-membrane domains; extra- and intracellular loops) of opsins were conducted online at graphpad.com. These tests used one degree of freedom and expected values were calculated under the assumption that sites inferred to be under positive selection are distributed randomly between the functional bipartitions (i.e., in proportion to the total number of sites in each partition). A significance level of $p = 0.05$ was applied.

Estimating visual pigment λ_{max}

It is possible, to some extent, to predict peak absorbance (λ_{max}) of visual pigments from amino acid sequences of their constituent opsins. Such predictions are possible because correlations exist between amino acid sequences of opsins and λ_{max} of corresponding pigments where this has been measured directly in photoreceptors or where opsin genes have been cloned and pigments regenerated *in vitro*. We made predictions of λ_{max} by assuming a vitamin A1 chromophore (A2 chromophores have not been reported in snakes (Davies et al. 2009, Hart et al. 2012, Schott et al. 20152016, Sillman et al. 1997, Simões et al. 2015, 2016) and assessing combinations of amino acids at 'spectral tuning' sites known to be especially important in determining λ_{max} in other vertebrates (see Yokoyama 2008 and references cited therein). Predicting λ_{max} based on selected (spectral tuning) amino acid sites is somewhat controversial because additional tuning sites and different tuning mechanisms might remain undiscovered (Hauser et al. 2014). The limited MSP data published thus far for snake visual pigments generally match predictions based on known tuning sites in other vertebrates (e.g. Davies et al. 2009, Simões et al. 2015, 2016). However, we were unable to make confident λ_{max} predictions in cases in which we found spectral tuning amino acids (or combinations thereof) not reported in other vertebrates, or where they occur in other vertebrates but in pigments for which λ_{max} has not been measured.

Ocular media spectral transmission

We examined spectral transmission of lenses and spectacles. Corneas and humours were not scanned because, with the exception of some fish corneas (Kondrasiv et al. 1986; Douglas and McGuigan 1989; Siebeck and Marshall 2000), the vertebrate lens always removes more shortwave radiation than either the cornea or humours (Douglas and Marshall 1999; Douglas and Jeffery 2014). Lenses, and some spectacle samples were thawed and briefly rinsed in phosphate-buffered saline (PBS) and mounted in purpose-built holders in air in front of a Shimadzu ISR 260 integrating sphere within a Shimadzu UV-2101PC spectrophotometer. Transmission at 700 nm was set to 100% and ocular media scanned at 1 nm intervals from 300 to 700 nm. We averaged the measurements of both eyes unless we had only one usable spectacle scale or lens. The lenses were small, 1–3 mm diameter (SI Table S22), limiting the amount of light transmitted through the measuring system, and the use on an integrating sphere reduced sensitivity further, thus the raw data are noisy at short wavelengths where lamp output is low. Data from scans were therefore smoothed using a cubic Savitzky-Golay filter (data frame length 51nm) using Matlab R2011a (The MathWorks Inc, MA, USA). The 50% cut-off wavelength ($\lambda_{50\%}$), the wavelength at which transmission is 50%, was determined for each sample and rounded to the nearest integer. The proportion of UVA (315–400 nm) transmission was calculated for each lens and spectacle following (Douglas and Jeffery 2014). $\lambda_{50\%}$ and %UVA values were plotted for primarily diurnal and

nocturnal species using the package ggplots2 (Wickham 2010) implemented in R (Team 2014) (R Core Team, 2014).

Results

We sequenced approximately 1100bp of cDNA for each of the three visual opsin genes, *sws1*, *lws* and *rh1* found in 48 snake species. Almost the entire coding region for *sws1*, *lws* and *rh1* was amplified and sequenced in the vast majority of species newly sampled. We amplified *rh1* in *Boiga ceylonensis* and *Macroprotodon brevis* (based on single gel bands of approximate expected fragment size) and perhaps *Phyllorhynchus decurtatus* (occasional multiple gel bands in 10 PCRs with various primer and annealing temperature combinations) but sequencing failed. We failed to amplify *rh1* in *Malpolon monspessulanus, sws1* in *Pareas monticola, Boiga ceylonensis* and *B. forsteni,* and *lws* in *Melanophidium khairei* and *Pareas monticola.* In each case between four and fourteen PCRs were repeated using various combinations of primers and annealing temperatures. With one exception (*M. monspessulanus*), the lack of amplification in the latter cases occurred in samples in which the cDNA was temporarily dehydrated, so the failed PCRs may be an artefact. With the addition of the visual opsin gene cDNA sequences previously published for other snakes, the dataset includes 69 snake species covering most major lineages, and representing a broad range of ecologies and retinal anatomies. Spectral transmission was determined for lenses and spectacles of 18 and 15 snake species, respectively.

Functionality and spectral sensitivity

The residues present at amino acid sites of known functional importance for spectral tuning of the visual pigments are reported in SI Tables S3–5. Predictions of visual pigment λ_{max} values are based on the assumed presence of a vitamin A1-derived chromophore; an A2 chromophore is not known in snakes but has been reported for some lizards (e.g. Martin et al. 2015). For *rh1* sequences, substitutions N83D and A292S are widespread across snake evolutionary history with multiple independent origins and reversals in Colubridae, Elapidae and Lamprophiidae (SI Table S3). The ancestral snake is reconstructed as having an RH1-based pigment with predicted λ_{max} of 493 nm. However, the ancestral colubrine and colubrid *rh1* sequences encode a combination of N83 and S292 (seen in several extant colubroids: Fig. 1), For *lws*In *Heterodon nasicus,* an A308S substitution is observed; this substitution is also found in combination with A180 in the mouse and rat LWS sequences (Davies et al. 2012) and in a number of aquatic mammals

(Newman and Robinson, 2006). The introduction of a S308A substitution by site directed mutagenesis in mouse LWS produces a 20 nm long-wave shift (Davies et al. 2012), so the presence of S308 in *H. nasicus* produce a short-wave shift. Ancestors of most major snake lineages are reconstructed as having an LWS pigment λ_{max} of 555 nm, with shifts to shorter wavelength λ_{max} occurring independently on multiple occasions within Colubridae (Fig. 1, SI Table S5).

Phylogenetics

The inferred *rh1* and *sws1* trees (SI Figs. S6–S11) are broadly consistent with recently published snake phylogenies estimated using more neutral markers, irrespective of whether analyses were run using ML or BI or under GTR+G or GTR+G+I. Notable exceptions to relationships found in recent molecular phylogenies of snakes are the nesting of *Lampropeltis* within dipsadine rather than colubrine colubrids (*rh1*), monophyly of the Scolecophia (*rh1*), and non-monophyly of Anomalepididae (*rh1*) and Lamprophiidae (*rh1*, *sws1*). The *lws* tree is less well supported and lacks some monophyletic higher taxa (e.g., Dipsadinae, Natricinae, Colubrinae, Colubroidea) present in the *rh1* and *sws1* trees. *Xylophis* (not sampled in molecular snake phylogenies) is recovered variably as closely related to some natricines (*lws*) or lying outside most colubroids (*rh1, sws1*).

Adaptive molecular evolution

Values for dN/dS (ω) (SI Table S12) suggest that all three visual opsin genes are under purifying selection (ω_{Rh1}= 0.237; ω_{SWS1}= 0.107; ω_{LWS}= 0.312), indicative of strong functional constraint (Li et al. 1985). Additional tests performed with alternative phylogenetic relationships among dipsadine, colubrine and natricine colubrids yield ω estimates that are not significantly different (data not shown), indicating that these results are robust with respect to this phylogenetic uncertainty.

For the *sws1* opsin gene, branch models (SI Table S12) suggest that non-fossorial (0.112), non-arboreal (0.08), non-aquatic (0.308) and diurnal (0.149) snake lineages have higher ω values then their counterparts (0.062, 0.097, 0.092 and 0.099, respectively). Colubrids have higher ω values (0.119) than non-colubrids (0.088). In the dataset pruned to species for which retinal anatomy is known, ω values are similar between taxa with (0.117) and without (0.101) transmuted cones, and lower in species with doubles cones (0.097 vs 0.110). The free-ratio model ω values vary between 0.001 and 0.409.

For the *lws* opsin gene ω values are higher in non-fossorial (0.340), arboreal (0.398), non-aquatic (0.308) and diurnal snakes (0.342) than their counterparts (0.016, 0.284, 0.268 and 0.246, respectively). Colubrids have significantly higher ω values (0.422) than non-colubrids (0.193). Higher ω occur in species with transmuted cones (0.543 vs. 0.273) and in species with double cones (0.373 vs 0.245). The free-ratio ω ranges from 0.001–7.1 (SI Table S12).

The *rh1* ω ratios among non-fossorial (0.252), non-arboreal (0.240), aquatic/semiaquatic (0.253) and nocturnal (0.240) snake lineages are higher than for their counterparts (0.161, 0.212, 0.0.229 and 0.141, respectively). Colubrids have higher (0.252) ω ratios than non-colubrids (0.212) whereas ω ratios are lower for the thoroughly fossorial Scolecophidia (0.141) than their sister group Alethinophidia (0.244). The *rh1* opsin gene is inferred to be under less functional constraint in snakes with transmuted, rod-like cones (0.388 vs. 0.212) and in snakes with double cones (0.283 vs 0.190) (SI Table S12).

The free-ratio ω ranges from 0.001–1.73, suggesting positive selection (ω = 1.44) in the Colubridae stem. With branch models, for all opsin genes, separate values for each of the contrasted ecologies and retinal types are a significantly better fit than a single ω value for all snakes when compared by LRT (SI Table S12).

Site models results infer several instances of positive selection at the codon level across the three visual opsin genes present in snakes (SI Table S13). Models 2a and M8 (β&ω) are significant better fit when compared with the simpler models M1a and M7, respectively (SI Table S13)

According to Bayes Empirical Bayes (BEB) implemented in site models M2a and M8 (β&ω) there are two and seven *sws1* amino acid sites that can be inferred to be under positive selection, respectively (SI Table S14). With M8 (β&ω), two of these seven sites (86 and 93) are known to have a substantial impact on SWS1 spectral tuning, and five of the sites are located in trans-membrane (TM) domains (Fig. 2). In *lws*, BEB results infer 12 and 18 amino acid sites under positive selection under models M2a and M8 (β&ω), respectively. Among the 18, two are involved in LWS spectral tuning and two others are located within the retinal pocket (Fig. 2). A total of 15 of the 18 inferred positively selected sites are located in TM domains, particularly TM 3, 4 and 5 (11 sites). In *rh1*, positive selection is inferredd in 11 and 16 amino-acid sites according to M2a and M8 (β&ω) models, respectively. Under model M8 (β&ω), BEB results infer positive selection in spectral sites 83 and 292 and in two sites within the retinal pocket (Fig. 2, SI Table S14). The majority of the *rh1* amino acids inferred to be under positive selection are located in TM domains, especially TM 3, 4, 5 and 7 (Fig. 2). For the results of both M2a and M8 (β&ω) models, chi-squared tests rejected the null that inferred positively

selected sites are not located within TMs versus loops more than expected for RH1 and LWS but not for SWS1. Pooling all visual opsins, chi squared-tests also rejected the null hypothesis that inferred positively selected sites are not located within extracellular versus intracellular loops more than expected.

Using PRIME (SI Table S16-S21), positive selection is inferred at amino acid sites at which substitutions with changes in biochemical properties occurred. Among these sites are spectral tuning sites 86 in *sws1* and 180 in *lws*, and amino acid sites situated within the retinal pocket in *lws* and *rh1* (Fig 2).

Ocular media transmission

The sampled snakes have lenses with a broad range of transmission properties at short wavelengths, ranging from those that filter out all of the UV and even some of blue (the lenses thus appearing yellow) to those that transmit most of the UVA (Fig 3A: SI Table S22). All spectacles transmitted the UVA well (Fig 3B), corroborating recent work on 42 snake species by van Doorn and Sivak (2015). All nocturnal species have very UVA transmissive lenses, while all species with lenses that cut out shorter wavelengths to varying degrees are diurnal (Fig 3C). However, not all snakes with some diurnal activity have UV-blocking lenses.

Discussion

Walls (1934; 1942) and Underwood (1967) documented extensive diversity in retinal anatomy among snakes. Our results demonstrate that snakes also display remarkable diversity in spectral transmission of the lens and variability in visual opsin gene sequences and visual pigment spectral sensitivity that together point to an evolutionarily complex system.

It has been argued that snakes passed through a nocturnal and/or fossorial stage early in their evolutionary history, with some associated diminution of their visual systems (see Simões et al. 2015) followed by possible re-elaboration in ‘higher’ snakes (Alethinophidia), including substantial diversification in retinal photoreceptor complements, at least at a morphological level (Walls 1942; Underwood 1967). The results presented here indicate that the complement of visual pigments, in contrast, has remained largely stable through notable evolutionary events such as the acquisition of double cones, the loss of classes of single cone (and perhaps rods), and the transmutations of both rods and cones.

The vast majority of species surveyed express the same three (*rh1, sws1, lws*) visual opsin genes that were likely to have been present in the ancestral snake (Davies et al. 2009; Simões et al. 2015). A striking feature is however the absence of *rh1* in the *Malpolon monspessulanus*. Given the good quality of the template cDNA available for this species, this is unlikely to be a PCR artefact. *Malpolon monspessulanus*, a highly diurnal species, is reported to have only cones (Underwood 1967; Underwood 1970) and a previous microspectrophotometric (MSP) study (Govardovskii and Chkheidze 1989) failed to find any visual pigments with a λ_{max} close to the c. 500 nm expected for RH1 pigments (typically occurring in rods). The presence of *rh1* in two other colubrids, *Phyllorhynchus decurtatus* and *Macroprotodon brevis* remains unconfirmed. *Phyllorhynchus decurtatus* is nocturnal but its 'rods' have been argued to be transmuted (rod-like) cones (Walls 1934), consistent therefore with the lack of RH1. Among vertebrates, absence of an expressed *rh1* has previously been reported only in another group of squamate reptiles, geckos (e.g. Loew et al. 1996; Yokoyama and Blow 2001). More work examining the physiology of visual pigments and gene expression will be required to test this further for snakes. Among those snakes with three functional visual opsin genes is *Uropeltis* cf. *macrolepis*. Like all uropeltids, this is a mostly fossorial species, though it is more likely to be seen above ground during daylight (D.J.G., pers. obs.) and has a larger eye than the distantly related, but also burrowing, scolecophidians and *Anilius scytale*, for which Simões et al. (2015) failed to amplify either *sws1* or *lws*. The presence of *sws1* and *lws* in *U.* cf. *macrolepis* adds support to Simões et al. (2015) conclusion that loss of all visual opsins except *rh1* has occurred in snakes in only the most dedicated of burrowers, and that if the ancestral snake was a burrower it was likely not as fossorial as living scolecophidians.

We predict that in snakes where the ocular media filter out most of the UVA (Fig 3A&B, SI Table S22), the SWS1 pigment λ_{max} is long-wave shifted. However, the *sws1* sequences of these species include previously unreported amino acid residues at some key tuning sites and direct measurements of visual pigment absorbance (e.g. by MSP) are currently lacking. Nevertheless, evidence from other studies (Carvalho et al. 2012; Cowing et al. 2002; Hunt and Peichl, 2014; Parry et al. 2004; Yokoyama et al. 2005) suggests that the replacement of is sufficient to shift the λ_{max} from UV to violet. only six of the 60 snakes listed in Table S4 may have lost a UVS SWS1 pigment. Removal of UV has been linked to increased acuity rather than an adaptation underpinning a particular form of colour vision or protection from harmful UV light (Douglas and Jeffery 2014). This hypothesis receives support here because the snakes with the least transparent lenses are highly visual hunters. These include a gliding species (*Chrysopelea ornata*) known to track distant objects (Socha and Sidor 2005) and a taxon (*Ahaetulla*) with horizontal pupils, binocular vision and a fovea (Walls 1942). The latter structure is

known from very few snakes (Rasmussen 1990) and is indicative of high visual acuity in a specialised area of the retina.

Based on ancestral state reconstruction for the *sws1* gene (and predictions of λ_{max}), the most recent common ancestor of living snakes was UV sensitive, and UV vision is also predicted to be present in many nocturnal caenophidians, matching the situation in other vertebrate groups (e.g., Veilleux and Cummings 2012) in which nocturnality is associated with UV sensitivity. Although there is evidence of a substantial amount of evolutionary change in snake *sws1* sequences, it is not possible to predict the λ_{max} of the SWS1-based visual pigments in 42 of the 63 species for which sequences are available (many of these species are not primarily nocturnal) because of tuning site amino acid substitutions (or combinations of substitutions) not known in other vertebrates. It is very likely (based on lens transmission) that at least some of these species have substantially long-wave shifted SWS1-based visual pigments. Hart et al. (Hart et al. 2012) found (using MSP) that the probable SWS1-based pigments in two sea snakes is not maximally sensitive in the UV, with λ_{max} of c. 429nm. Although many snakes have previously unknown *sws1* tuning site substitutions, there is evidence that some sequences discovered here produce substantial changes in SWS1 $\lambda_{max.}$ Mutations at site 86 are known to cause major shifts in SWS1 λ_{max}, with F86Y (Fasick and Robinson 1998; Cowing et al. 2002) and F86S (Shi et al. 2001) short-wave shifting λ_{max} by 66 and 51 nm (Yokoyama 2005) respectively, and the latter mutation is observed in the snakes *Malpolon monspessulanus* and *Pantherophis guttatus.* In *Ahaetulla nasuta*, *Chrysopelea ornata*, *Helicops angulatus* and *Chironius* spp. F86V is observed. The guinea pig has a 86V substitution and an SWS1 λ_{max} of 420nm and, furthermore, the V86F substitution produces one of the most substantial shifts towards the UV with a decrease of 53nm in the SWS1 pigment λ_{max} (Parry et al. 2004). Given the filtering out of UV light by the lens a short-wave shifted λ_{max} would seem very unlikely, otherwise SWS1 would not function as an efficient visual pigment in these snakes.

In *Helicops angulatus*, cloning the *sws1* gene revealed polymorphism at site 86 with either valine or phenylalanine. The exact change in spectral tuning is not known, but, speculatively, this polymorphism indicates that pigments with spectral peaks in the UV and violet may be present simultaneously and potentially may therefore provide the basis for a form of trichromacy. This would be similar to the form of trichromacy in polymorphic female platyrrhine monkeys (Jacobs et al. 2002), if some random allele inactivation is present that ensures only one allele is expressed per photoreceptor. Alternatively, both alleles in *H. angulatus* may be fully active to give a broader spectrum of sensitivity.

In contrast to *rh1* and *sws1,* the *lws* spectral sites in snakes are identical to those known in other vertebrates, with the exception of the A308S substitution unique to the colubrine *Heterodon nasicus*. Variation in the amino acid residues at LWS spectral sites in snakes suggests multiple LWS λ_{max} shifts between long (555-560nm) and medium wavelengths (536nm) within Caenophidia. Substitutions are particularly common in Dipsadinae and Colubrinae, with most shifts to predicted shorter wavelength λ_{max} values occurring in nocturnal taxa, thereby providing a possible adaptation to maximize photon capture and potentially colour vision in low light conditions. In a study of forest mammals, Veilleux and Cummings (2012) found that SWS spectral tuning appeared to be strongly associated with foraging target and LWS tuning to dominant light field characteristics. Although the shorter wavelength shifted LWS λ_{max} values of nocturnal snakes match this, we are unable to address whether snake SWS1 is more tuned to foraging targets because SWS1 λ_{max} is not known for most snakes (see above), dietary classification is non-trivial, and many snakes are probably primarily using olfaction rather than visual clues to detect prey

The results of our analyses of positive selection in snake visual opsins are notable on two counts. Firstly, unlike some other studies of vertebrate visual opsins (e.g. Yokoyama et al. 2008) we infer multiple sites as under positive selection in all three visual opsins and some of these occur in sites of known functional importance, including known spectral tuning sites. This is consistent with the interpretation that the tuning of snake LWS pigments is influenced by positive selection at sites known to be important in effecting tuning variation in many other vertebrate groups (Hunt and Collin 2014). Secondly, shifts in the molecular evolution (functional constraint) of the visual pigment genes are correlated with many variables, including ecological niche characteristics and retinal anatomy. That the inferred functional constraint is lower in all visual opsin genes in snakes with transmuted, rod-like cones is an important observation indicating that visual pigment adaptation occurs in association with morphological transmutation of photoreceptors — an incompletely understood process with poorly known functional outcomes (Simões et al. 2016). Although we found evidence for less functional constraint in the evolution of *rh1* and *lws* (but not *sws1*) in lineages with double cones, this is difficult to interpret because the function of double cones remains largely unknown (e.g. Pignatelli et al. 2010).

Of the three visual opsins found in snakes, *sws1* has fewer amino acid sites inferred to be under positive selection, consistent with higher purifying selection estimates on branch models (SI Table S12) and possibly indicating possibly greater purifying selection than in *lws* and *rh1*. This is consistent with the relatively few tuning sites identified in SWS1 opsins. Indeed, two of the seven *sws1* sites inferred to be under

positive selection are the spectral tuning sites 86 and 93 known to impart substantial λ_{max} shifts (Fasick and Robinson 1998; Shi et al. 2001; Yokoyama 2005), suggestive of at least some localized positive selection on sites of functional importance. Similarly, *lws*, sites 180 and 285 and *rh1* sites 83 and 292 are inferred to be under positive selection and also mediate important changes in λ_{max} of their respective pigments (see above). Thus, some of the evolution of snake visual opsins inferred here is interpreted as likely adaptive change related to spectral tuning of pigments. Colour vision has yet to be demonstrated behaviourally in snakes, but our results suggest it is almost certainly an important part of their sensory biology, especially for many caenophidians. The visual pigment complement of most snakes, comprising RH1, SWS1 and LWS based pigments, is strongly suggestive of photopic cone dichromacy and scotopic monochromacy as found in most mammals. However, there remains the possibility of trichromacy, either by the involvement of transmuted cone-like rods in the case of diurnal species (Schott et al. 2016), or by the use of transmuted rod-like cones in nocturnal species (as occurs in geckos: Roth & Kelber 2004). As with the observed polymorphism of *sws1* found in *Helicops angulatus*, further studies are required to elucidate these possibilities and the consequences of different visual pigment complements in snake colour vision.

Most of the amino acid sites inferred to be under positive selection in the three visual opsin genes found in snakes are in transmembrane domains (Fig. 3), and most observed changes at these sites are non-conservative in terms of amino acid properties (Fig. 2, SI Table S13). Transmembrane domains impact the tertiary structure, thermal stability (Kobilka 2007) and aspects of the retinal binding pocket (Yokoyama et al. 2006) of the opsin, such that positive selection at these sites is likely to have major influence on opsin function. Change in spectral tuning is only one of the possible functional outcomes of visual opsin amino acid substitutions - there is more to visual pigments than spectral absorption - and these other aspects of visual sensory transduction will need to be part of the future investigations of this system.

Conclusion

Based on surveys of retinal anatomy, the eyes of snakes have been cited as one of the most interesting cases of visual adaptation among vertebrates (Walls 1942; Underwood 1967), but they remained overlooked during the revolution in molecular analyses of visual pigment genes. Our results show that in addition to the substantial anatomical diversity, snakes also have notable diversity in their lens transmission and visual opsin genes, including diversity not known in other vertebrates, and these aspects of snake vision are shown to have undergone considerable evolution. Snake visual opsin

genes contain signals of positive selection in sites of functional importance that are (perhaps causally) associated with shifts in ecology and retinal anatomy. We conclude that the diversity, function and evolution of snake vision are worthy of additional research, and that understanding of vertebrate vision is incomplete without a consideration of snakes.

Acknowledgements

This work was funded by a grant from the Leverhulme Trust (RPG-342 to DJG, NSH, DMH & JCP). Permits for research and export were granted by Direction de l'Environment de l'Aménagement et du Logement and the Direction des Services Vétérinaires de la Guyane, Cayenne, French Guiana, and by the Ministry of Forestry & Wildlife of Cameroon. For assistance in the field, we thank Gabriela Bittencourt-Silva, Antoine Fouquet, Philippe Gaucher, Jeannot and Odette (Camp Patawa) and Mark Wilkinson. Additional practical assistance with obtaining and processing samples, and with literature and analysis was provided by Christian Cox, Vivek Philip Cyriac, David Donaire, Robert Fisher, Varad Giri, Rachunliu G. Kamei, Panagiotis Kornilios, Marcel Kouete, Dileep Kumar, Michelle Lawing, Mruganka Rahul Lele, Gopal Murali, Jesse Meik, Simon Maddock, Bartosz Nadol, David Richards, Gill Sparrow, Jeff Streicher, Colin Strine, Ed Wade, Chris Williamson, Mark Wilkinson, and the NHM Sequencing Facility, and we thank them all. Chris Hull provided help with the smoothing of the ocular media transmission data.

References

Atchley WR, Zhao J, Fernandes AD, Drüke T. 2005. Solving the protein sequence metric problem. *Proc Natl Acad Sci. USA*. 102:6395–6400.

Bowmaker J, Hunt D. 2006. Evolution of vertebrate visual pigments. *Curr Biol.* 16:R484–R849.

Carleton KL, Hofmann CM, Klisz C, Patel Z, Chircus LM, Simenauer LH, Soodoo N, Albertson RC, Ser JR. 2010. Genetic basis of differential opsin gene expression in cichlid fishes. *J Evol Biol.* 23:840–853.

Conant GC, Wagner GP, Stadler PF. 2007. Modeling amino acid substitution patterns in orthologous and paralogous genes. *Mol Phyl and Evol.* 42:298–307.

Cowing JA, Poopalasundaram S, Wilkie SE, Robinson PR, Bowmaker JK, Hunt DM. 2002. The molecular mechanism for the spectral shifts between vertebrate ultraviolet- and violet-sensitive cone visual pigments. *Biochem J.* 367:129.

Darriba D, Taboada GL, Doallo R, Posada D. 2012. jModelTest 2: more models, new

heuristics and parallel computing. *Nat Methods.* 9:772.

Davies WIL, Collin SP, Hunt DM. 2012. Molecular ecology and adaptation of visual photopigments in craniates. *Mol Ecol.* 21:3121–3158.

Davies WL, Cowing JA, Bowmaker JK, Carvalho LS, Gower DJ, Hunt DM. 2009. Shedding Light on Serpent Sight: The Visual Pigments of Henophidian Snakes. *J Neurosci.* 29:7519–7525.

Delport W, Poon AFY, Frost SDW, Kosakovsky Pond SL. 2010. Datamonkey 2010: a suite of phylogenetic analysis tools for evolutionary biology. *Bioinformatics*. 26:2455–2457.

Delport W, Scheffler K, Botha G, Gravenor MB, Muse SV, Kosakovsky Pond SL. 2010. CodonTest: Modeling Amino Acid Substitution Preferences in Coding Sequences. *PLoS Comput Biol.* 6:e1000885.

Douglas RH, Jeffery G. 2014. The spectral transmission of ocular media suggests ultraviolet sensitivity is widespread among mammals. *Proc R Soc. B* 281:20132995–20132995.

Douglas RH, Marshall NJ. 1999. A review of vertebrate and invertebrate ocular filters. In: Adaptive Mechanisms in the Ecology of Vision. Dordrecht: Springer Netherlands. pp. 95–162.

Douglas RH, McGuigan CM. 1989. The spectral transmission of freshwater teleost ocular media – an interspecific comparison and a guide to potential ultraviolet sensitivity. *Vision Res.* 29:871–879.

Dulai K, Dornum M, Mollon J, Hunt D. 1999. The Evolution of Trichromatic Color Vision by Opsin Gene Duplication in New World and Old World Primates. *Genome Res.* 9:629–638.

Edgar, RC. 2004. MUSCLE: multiple sequence alignment with high accuracy and high throughput. *Nucleic Acids Res*. 32: 1792–1797.

Enright JM, Toomey MB, Sato S-Y, Temple SE, Allen JR, Fujiwara R, Kramlinger VM, Nagy LD, Johnson KM, Xiao Y, et al. 2015. Cyp27c1 Red-Shifts the Spectral Sensitivity of Photoreceptors by Converting Vitamin A1 into A2. *Curr Biol.* 25: 1-10.

Fasick JI, Robinson PR. 1998. Mechanism of spectral tuning in the dolphin visual pigments. *Biochemistry* 37:433–438.

Gans C, Fetcho JR. 1982. The Sri Lankan genus Aspidura (Serpentes, reptilia, Colubridae). *Annals of Carnegie Museum* 51(14): 271–316.

Govardovskii VI, Chkheidze NI. 1989. Retinal photoreceptors and visual pigments in

686 certain snakes. *Biol Abstr.* 90:1036.

687 Gower DJ, Winkler JD. 2007. Taxonomy of the Indian snake Xylophis Beddome
688 (Serpentes: Caenophidia), with description of a new species. *Hamadryad* 31:315–329.

689 Hart NS, Coimbra JP, Collin SP, Westhoff G. 2012. Photoreceptor types, visual pigments,
690 and topographic specializations in the retinas of hydrophiid sea snakes. *J Comp Neurol*.
691 520:1246–1261.

692 Hauser FE, van Hazel I, Chang BSW. 2014. Spectral tuning in vertebrate short
693 wavelength-sensitive 1 (SWS1) visual pigments: Can wavelength sensitivity be inferred
694 from sequence data? *J Exp Zool B Mol Dev Evol.* 322:529–539.

695 Hofmann CM, Carleton KL. 2009. Gene Duplication and Differential Gene Expression Play
696 an Important Role in the Diversification of Visual Pigments in Fish. *Integr Comp Biol.*
697 49:630.

698 Huelsenbeck JP, Ronquist F. 2001. MRBAYES: Bayesian inference of phylogenetic trees.
699 *Bioinformatics* 17:754–755.

700 Hunt DM, Collin SP. 2014. Evolution of Visual and Non-visual Pigments. In: Hunt DM,
701 Hankins MW, Collin SP, Marshall NJ, editors. Evolution of Visual and Non-visual
702 Pigments. Boston, MA: Springer. p. 276.

703 Hunt DM, Dulai KS, Partridge JC, Cottrill P, Bowmaker JK. 2001. The molecular basis for
704 spectral tuning of rod visual pigments in deep-sea fish. *J Exp Biol.* 204:3333–3344.

705 Jacobs G, II J, Tan Y, Li W-H. 2002. Opsin gene and photopigment polymorphism in a
706 prosimian primate. *Vision Res.* 42:11–18.

707 Janz JM, Farrens DL. 2001. Engineering a Functional Blue-Wavelength-Shifted Rhodopsin
708 Mutant†. *Biochemistry* 40:7219–7227.

709 Katoh K, Misawa K, Kuma K, Miyata T. 2002. MAFFT: a novel method for rapid multiple
710 sequence alignment based on fast Fourier transform. *Nucleic Acids Res.* 30:3059–3066.

711 Kearse M, Moir R, Wilson A, Stones-Havas S, Cheung M, Sturrock S, Buxton S, Cooper A,
712 Markowitz S, Duran C, et al. 2012. Geneious Basic: an integrated and extendable
713 desktop software platform for the organization and analysis of sequence data.
714 *Bioinformatics* 28:1647–1649.

715 Kobilka BK. 2007. G protein coupled receptor structure and activation. *BBA -*
716 *Biomembranes* 1768:794–807.

717 Kondrasiv SL, Gamburzena AG, Gnjibkina VP, Orlov OJ, My PT. 1986. Coloration of
718 corneas in fish. A list of species. *Vision Res.* 26:287–290.

719 Land MF. 1981. Optics and vision in invertebrates. In: Autrum HJ, editor. Handbook of
720 Sensory Physiology. Vol. VII/6B. Berlin. pp. 471–592.

721 Li WH, Wu CI, Luo CC. 1985. A new method for estimating synonymous and
722 nonsynonymous rates of nucleotide substitution considering the relative likelihood of
723 nucleotide and codon changes. *Mol Biol Evol.* 2:150–174.

724 Loew ER, Govardovskii VI, Rohlich P, Szél A. 1996. Microspectrophotometric and
725 immunocytochemical identification of ultraviolet photoreceptors in geckos. *Vis*
726 *Neurosci.* 13:247–256.

727 Löytynoja A & Goldman N. 2005. An algorithm for progressive multiple alignment of
728 sequences with insertions. *Proc Nat Acad Sci USA*. *102*(30): 10557–10562.

729 Martin M, Le Galliard J-F, Meylan S, Loew ER. 2015. The importance of ultraviolet and
730 near-infrared sensitivity for visual discrimination in two species of lacertid lizards. *J Exp*
731 *Biol.* 218:458–465.

732 McDowell SB. 1987. Systematics. In: Seigel RA, Collins JT, Novak SS, editors. Snakes:
733 Ecology and Evolutionary Biology. New York. MacMillan pp. 3–50.

734 Nathans J. 1990. Determinants of Visual Pigment Absorbance: Role of Charged Amino
735 Acids in the Putative Transmembrane Segments. *Biochemistry* 29:937.

736 Nickle B, Robinson PR. 2007. The opsins of the vertebrate retina: insights from
737 structural, biochemical, and evolutionary studies. *Cell Mol Life Sci.* 64:2917–2932.

738 Nilsson DE. 1996. Eye ancestry: old genes for new eyes. *Curr Biol.* 6:39–42.

739 Parry J, Poopalasundaram S, Bowmaker J, Hunt D. 2004. A Novel Amino Acid
740 Substitution Is Responsible for Spectral Tuning in a Rodent Violet-Sensitive Visual
741 Pigment. *Biochemistry* 43:8014–8020.

742 Pattengale ND, Alipour M, Bininda-Emonds ORP, Moret BME, Stamatakis A. 2009. How
743 Many Bootstrap Replicates Are Necessary? In: Springer-Verlag. pp. 184–200.

744 Pignatelli V, Champ C, Marshall J, Vorobyev M. 2010. Double cones are used for colour
745 discrimination in the reef fish, Rhinecanthus aculeatus. *Biol Lett.* 6:537–539.

746 Pyron R, Burbrink FT, Wiens JJ. 2013. A phylogeny and revised classification of
747 Squamata, including 4161 species of lizards and snakes. *BMC Evol Biol.* 13:93.

748 Rasmussen JB. 1990. The retina of Psammodynastes pulverulentus (Boie, 1827) and
749 Telescopus fallax (Fleischmann, 1831) with a discussion of their phylogenetic
750 significance (Colubroidea, Serpentes). *J Zool Syst Evolut.* 28:269–276.

751 Reeder TW, Townsend TM, Mulcahy DG, Noonan BP, Wood PL, Sites JW, Wiens JJ. 2015.
752 Integrated Analyses Resolve Conflicts over Squamate Reptile Phylogeny and Reveal
753 Unexpected Placements for Fossil Taxa. PLoS ONE 10:e0118199.

754 Schott RK, Müller J, Yang CGY, Bhattacharyya N , Chan N, Xu M, et al. . Evolutionary
755 transformation of rod photoreceptors in the all-cone retina of a diurnal garter snake.
756 *Proc Nat Acad Sci USA*. 201513284.

757 Shi Y, Radlwimmer FB, Yokoyama S. 2001. Molecular genetics and the evolution of
758 ultraviolet vision in vertebrates. *Proc Natl Acad Sci USA.* 98:11731–11736.

759 Siebeck UE, Marshall NJ. 2000. Transmission of ocular media in labrid fishes. *Phil. Trans.*
760 *Royal Soc B: Biol Sc.* 355:1257–1261.

761 Sillman AJ, Govardovskii VI, Rohlich P, Southard JA, Loew ER. 1997. The photoreceptors
762 and visual pigments of the garter snake (Thamnophis sirtalis): a
763 microspectrophotometric, scanning electron microscopic and immunocytochemical
764 study. *J Comp Physiol A* 181:89.

765 Simões BF, Sampaio FL, Jared C, Antoniazzi MM, Loew ER, Bowmaker JK, Rodriguez A,
766 Hart NS, Hunt DM, Partridge JC, et al. 2015. Visual system evolution and the nature of
767 the ancestral snake. *J Evol Biol.* 28:1309–1320.

768 Simões, B. F., Sampaio, F. L., Loew, E. R., Sanders, K. L., Fisher, R. N., Hart, N. S., et al.
769 2016. Multiple rod-cone and cone-rod photoreceptor transmutations in snakes:
770 evidence from visual opsin gene expression. *Proc R Soc.* B 283: 1823.

771 Stamatakis A. 2014. RAxML version 8: a tool for phylogenetic analysis and post-analysis
772 of large phylogenies. *Bioinformatics* 30:1312–1313.

773 Team RC. 2014. R: A language and environment for statistical computing. Vienna,
774 Austria: R Foundation for Statistical Computing

775 Thorpe A. 1991. Spectral trtansmission and short–wave absorbing pigments in the
776 lenses of fish and other animals. City University, London.

777 Underwood G. 1967. A Contribution to the Classification of Snakes. London: British
778 Museum Natural History Publications

779 Underwood G. 1970. The Eye. In: Gans C, Parsons TS, editors. Biology of the Reptilia:
780 Morphology B. Vol. 2. New York: Academic Press. pp. 1–97.

781 van Doorn K, Sivak JG. 2015. Spectral transmittance of the spectacle scale of snakes and
782 geckos. *Contrib Zool.* 8:1–12.

783 Veilleux CC, Cummings ME. 2012. Nocturnal light environments and species ecology:

784 implications for nocturnal color vision in forests. *J Exp Biol.* 215:4085–4096.

785 Wald G. 1968. The molecular basis of visual excitation. *Nature*. 219:800–807.

786 Walls GL. 1931. The Occurrence of Colored Lenses in the Eyes of Snakes and Squirrels,
787 and Their Probable Significance. *Copeia* 1931:125–127.

788 Walls GL. 1934. The reptilian retina. I. A new concept of visual cell evolution. *Am J*
789 *Ophthalmol.* 17:892–915.

790 Walls GL. 1942. The Vertebrate Eye and Its Adaptive Radiation. New York: Fafner
791 Publishing Company

792 Wickham H. 2010. ggplot2. New York, NY: Springer

793 Wiens JJ, Hutter CR, Mulcahy DG, Noonan BP, Townsend TM, Sites JW, Reeder TW.
794 2012. Resolving the phylogeny of lizards and snakes (Squamata) with extensive sampling
795 of genes and species. *Biol Lett.* 8:1043–1046.

796 Yang Z. 1998. Likelihood ratio tests for detecting positive selection and application to
797 primate lysozyme evolution. *Mol Biol Evol.* 15:568–573.

798 Yang, Z. 2006. Computational molecular evolution. Oxford University Press, USA.

799 Yang Z. 2007. PAML 4: Phylogenetic Analysis by Maximum Likelihood. *Mol Biol Evol.*
800 24:1586–1591.

801 Yang ZH, Nielsen R, Goldman N, Pedersen A. 2000. Codon-substitution models for
802 heterogeneous selection pressure at amino acid sites. *Genetics* 155:431–449.

803 Yang ZH, Wong W, Nielsen R. 2005. Bayes Empirical Bayes Inference of Amino Acid Sites
804 Under Positive Selection. *Mol Biol Evol.* 22:1107.

805 Yokoyama S, Blow NS. 2001. Molecular evolution of the cone visual pigments in the pure
806 rod-retina of the nocturnal gecko, Gekko gekko. *Gene* 276:117–125.

807 Yokoyama S, Starmer WT, Takahashi Y, Tada T. 2006. Tertiary structure and spectral
808 tuning of UV and violet pigments in vertebrates. *Gene* 365:95–103.

809 Yokoyama S, Tada T, Zhang H, Britt L. 2008. Elucidation of phenotypic adaptations:
810 Molecular analyses of dim-light vision proteins in vertebrates. *Proc Natl Acad Sci USA*.
811 105:13480–13485.

812 Yokoyama S, Xing J, Liu Y, Faggionato D, Altun A, Starmer WT. 2014. Epistatic Adaptive
813 Evolution of Human Color Vision. *PLoS Genet.* 10:e1004884.

814 Yokoyama S. 2005. Elephants and Human Color-Blind Deuteranopes Have Identical Sets

of Visual Pigments. *Genetics* 170:335–344.

Yokoyama S. 2008. Evolution of Dim-Light and Color Vision Pigments. *Annu Rev Genomics Hum Genet.* 9:259–282.

Zhang J. 2005. Evaluation of an Improved Branch-Site Likelihood Method for Detecting Positive Selection at the Molecular Level. *Mol Biol Evol.* 22:2472–2479.

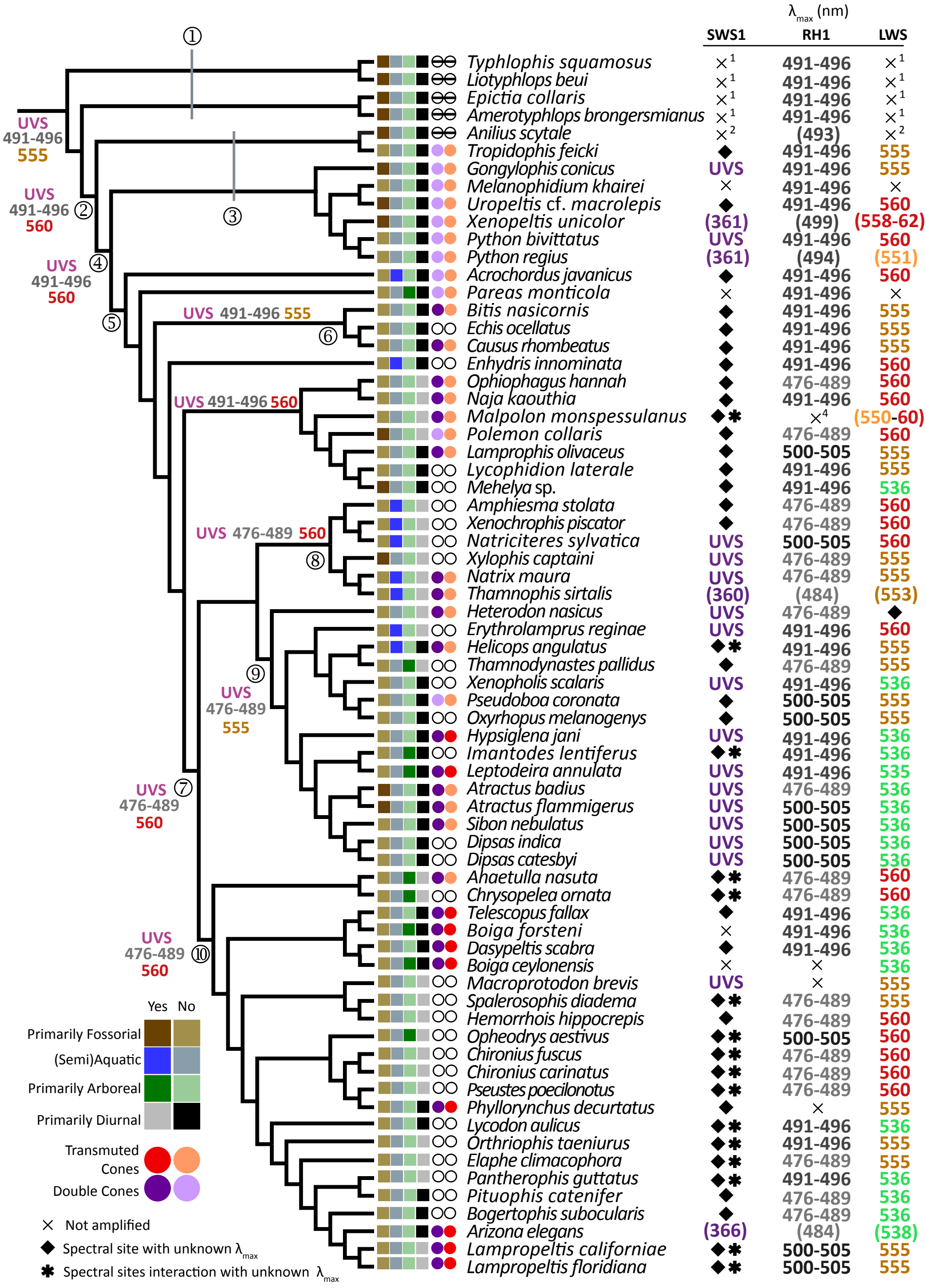
λmax (nm)
SWS1
RH1
LWS
UVS 491-496 555
UVS 491-496 560
UVS 491-496 560
UVS 491-496 555
UVS 491-496 560
UVS 476-489 560
UVS 476-489 555
UVS 476-489 560
UVS 476-489 560
① ② ③ ④ ⑤ ⑥ ⑦ ⑧ ⑨ ⑩
Typhlophis squamosus × 1 491-496 × 1
Liotyphlops beui × 1 491-496 × 1
Epictia collaris × 1 491-496 × 1
Amerotyphlops brongersmianus × 1 491-496 × 1
Anilius scytale × 2 (493) × 2
Tropidophis feicki ◆ 491-496 555
Gongylophis conicus UVS 491-496 555
Melanophidium khairei × 491-496 ×
Uropeltis cf. macrolepis ◆ 491-496 560
Xenopeltis unicolor (361) (499) (558-62)
Python bivittatus UVS 491-496 560
Python regius (361) (494) (551)
Acrochordus javanicus ◆ 491-496 560
Pareas monticola × 491-496 ×
Bitis nasicornis ◆ 491-496 555
Echis ocellatus ◆ 491-496 555
Causus rhombeatus ◆ 491-496 555
Enhydris innominata ◆ 491-496 560
Ophiophagus hannah ◆ 476-489 560
Naja kaouthia ◆ 491-496 560
Malpolon monspessulanus ◆✱ × 4 (550-60)
Polemon collaris ◆ 476-489 560
Lamprophis olivaceus ◆ 500-505 555
Lycophidion laterale ◆ 491-496 555
Mehelya sp. ◆ 491-496 536
Amphiesma stolata ◆ 476-489 560
Xenochrophis piscator ◆ 476-489 560
Natriciteres sylvatica UVS 500-505 560
Xylophis captaini UVS 476-489 555
Natrix maura UVS 476-489 555
Thamnophis sirtalis (360) (484) (553)
Heterodon nasicus UVS 476-489 ◆
Erythrolamprus reginae UVS 491-496 560
Helicops angulatus ◆✱ 491-496 555
Thamnodynastes pallidus ◆ 476-489 555
Xenopholis scalaris UVS 491-496 536
Pseudoboa coronata ◆ 500-505 555
Oxyrhopus melanogenys ◆ 500-505 555
Hypsiglena jani UVS 491-496 536
Imantodes lentiferus ◆✱ 491-496 536
Leptodeira annulata UVS 491-496 535
Atractus badius UVS 476-489 536
Atractus flammigerus UVS 500-505 536
Sibon nebulatus UVS 500-505 536
Dipsas indica UVS 500-505 536
Dipsas catesbyi UVS 500-505 536
Ahaetulla nasuta ◆✱ 476-489 560
Chrysopelea ornata ◆✱ 476-489 560
Telescopus fallax ◆ 491-496 536
Boiga forsteni × 491-496 536
Dasypeltis scabra ◆ 491-496 536
Boiga ceylonensis × × 536
Macroprotodon brevis UVS × 555
Spalerosophis diadema ◆✱ 476-489 555
Hemorrhois hippocrepis ◆ 476-489 560
Opheodrys aestivus ◆✱ 500-505 560
Chironius fuscus ◆✱ 476-489 560
Chironius carinatus ◆✱ 476-489 560
Pseustes poecilonotus ◆✱ 476-489 560
Phyllorynchus decurtatus ◆ × 555
Lycodon aulicus ◆✱ 491-496 536
Orthriophis taeniurus ◆✱ 491-496 555
Elaphe climacophora ◆✱ 476-489 555
Pantherophis guttatus ◆✱ 491-496 536
Pituophis catenifer ◆ 476-489 536
Bogertophis subocularis ◆ 476-489 536
Arizona elegans (366) (484) (538)
Lampropeltis californiae ◆✱ 500-505 555
Lampropeltis floridiana ◆✱ 500-505 555
Yes No
Primarily Fossorial
(Semi)Aquatic
Primarily Arboreal
Primarily Diurnal
Transmuted Cones
Double Cones
× Not amplified
◆ Spectral site with unknown λmax
✱ Spectral sites interaction with unknown λmax

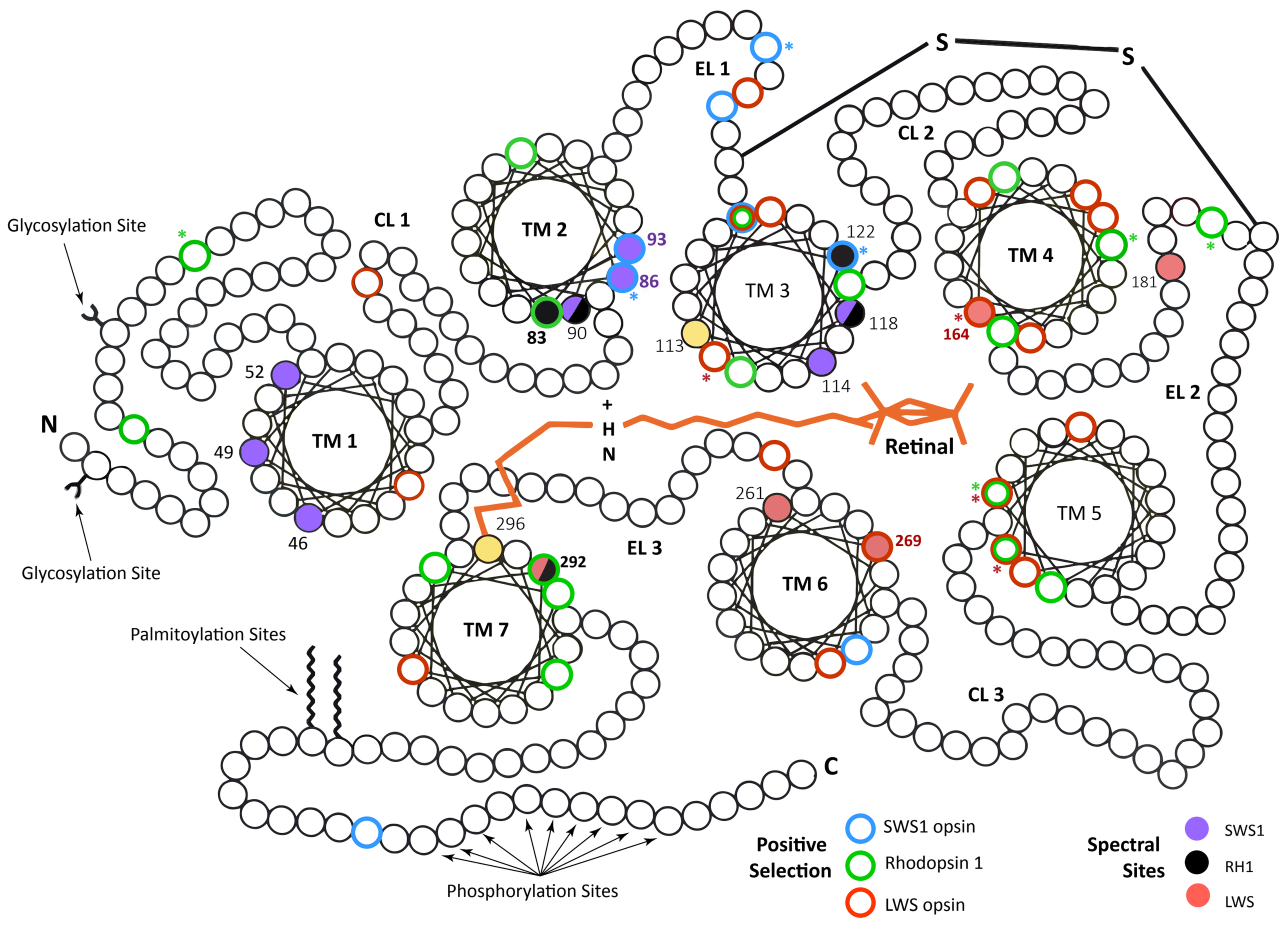
Glycosylation Site
CL 1
TM 2
EL 1
S
S
CL 2
TM 4
TM 3
122
118
113
114
164
181
EL 2
N
52
TM 1
49
46
Glycosylation Site
+
H
N
Retinal
261
269
296
292
EL 3
TM 6
TM 5
TM 7
CL 3
Palmitoylation Sites
C
Phosphorylation Sites
Positive Selection
SWS1 opsin
Rhodopsin 1
LWS opsin
Spectral Sites
SWS1
RH1
LWS

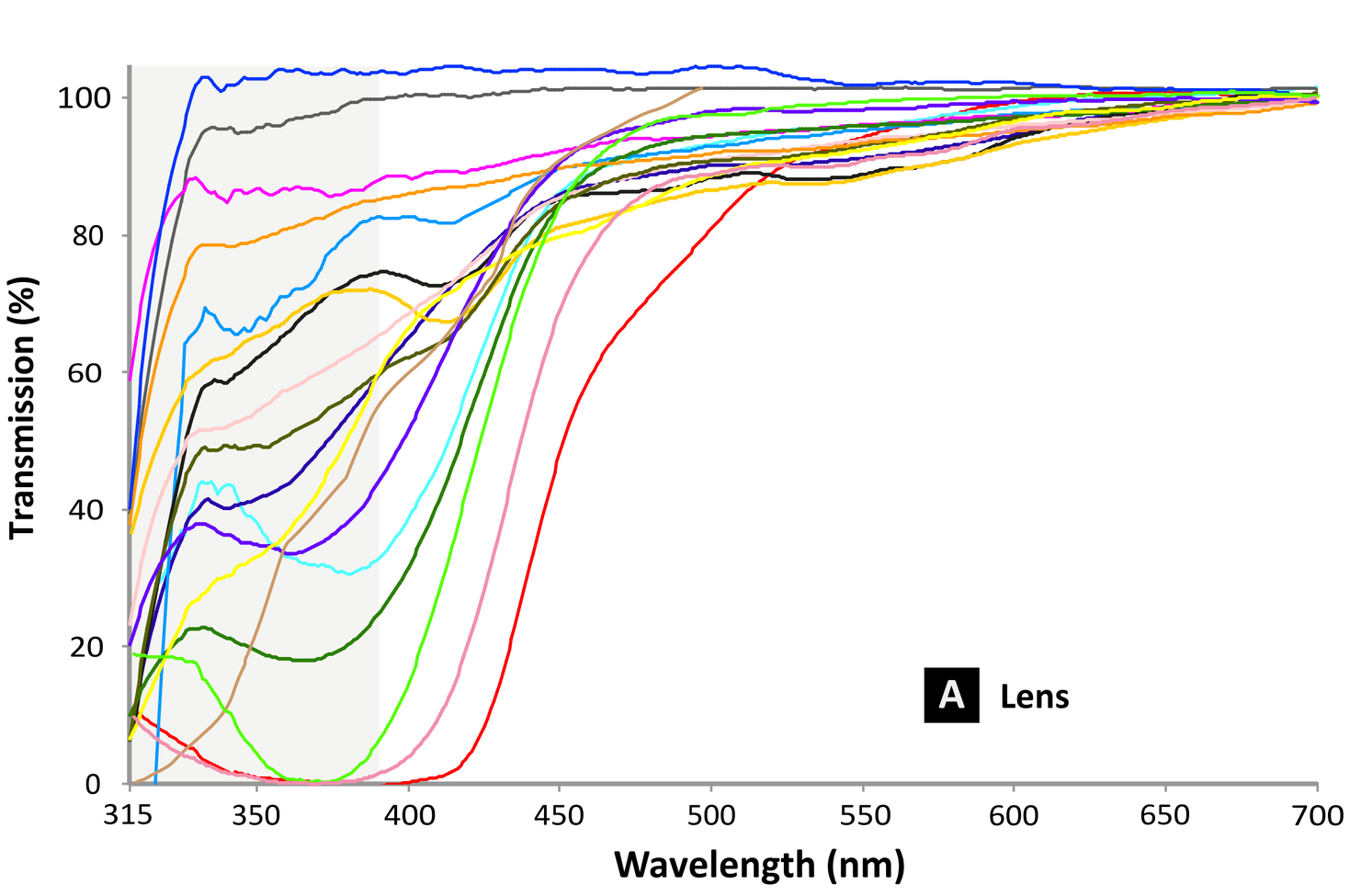
Transmission (%)
100
80
60
40
20
0
315
350
400
450
500
550
600
650
700
Wavelength (nm)
A Lens

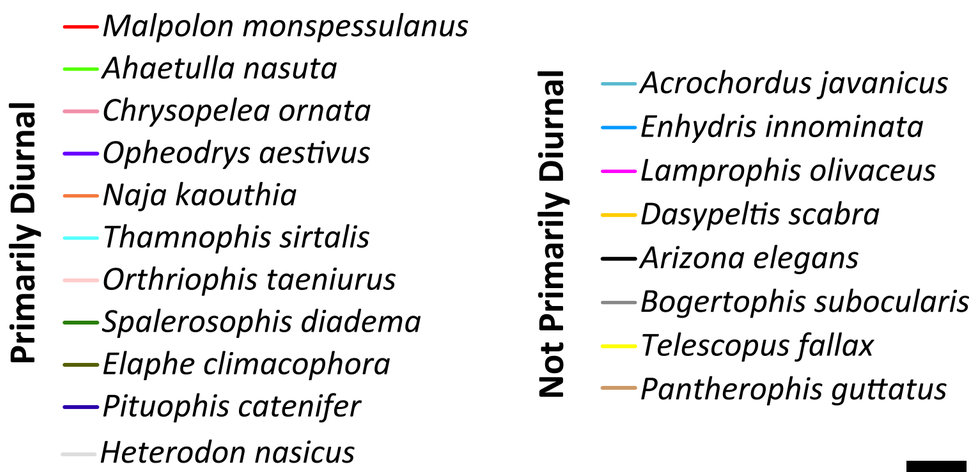
Primarily Diurnal
Malpolon monspessulanus
Ahaetulla nasuta
Chrysopelea ornata
Opheodrys aestivus
Naja kaouthia
Thamnophis sirtalis
Orthriophis taeniurus
Spalerosophis diadema
Elaphe climacophora
Pituophis catenifer
Heterodon nasicus
Not Primarily Diurnal
Acrochordus javanicus
Enhydris innominata
Lamprophis olivaceus
Dasypeltis scabra
Arizona elegans
Bogertophis subocularis
Telescopus fallax
Pantherophis guttatus

Transmission (%)
100
80
60
40
20
0
315
350
400
450
500
550
600
650
700
Wavelength (nm)
UV
Visible
B Spectacle

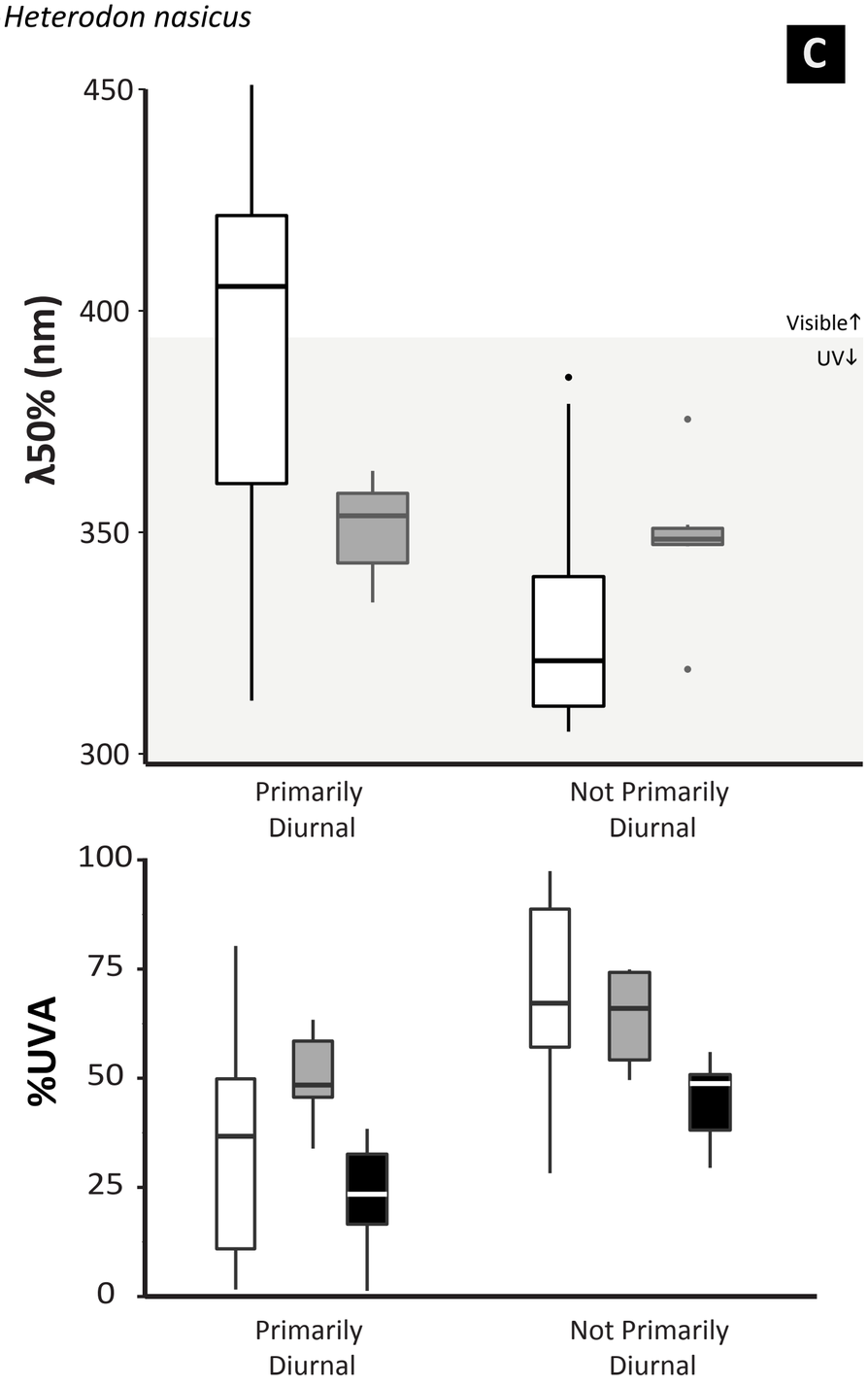
C
λ50% (nm)
450
400
350
300
Visible↑
UV↓
Primarily Diurnal
Not Primarily Diurnal
%UVA
100
75
50
25
0
Primarily Diurnal
Not Primarily Diurnal

FIGURE CAPTIONS

Figure 1. Snake species tree and phenotypic classifications (see Material and Methods for more information) used in analyses of opsin gene evolution. Numbers within circles represent snake higher taxa: ①Scolecophidia (not recovered in some molecular phylogenies); ②Alethinophidia; ③Henophidia (not recovered in molecular phylogenies); ④ Afrophidia; ⑤ Caenophidia; ⑥Viperidae; ⑦Colubridae, ⑧Natricinae ⑨Dipsadinae; ⑩Colubrinae. Phenotype classifications shown for ecology (squares) and visual cell patterns (circles), with empty circles representing species for which state is unknown and strikethrough circles species with retinas with no cones. Visual pigment peak absorbance (λ_{max}) values for each visual pigment are those predicted from cDNA sequences except where indicated. Ancestral pigment λ_{max} values are shown at selected internal branches in order SWS1-RH1-LWS. 1) SWS1 and LWS pigments have not been detected by MSP for any scolecophidian, and no cones have been found in anatomical studies (see Simões et al. 2015); 2) Anatomical studies have not been carried out for *Anilius scytale* but MSP in this species detected only a single visual pigment (RH1: Simões et al. 2015); 3) No visual pigment with an RH1-like λ_{max} was detected by MSP for *Malpolon* (Govardovski & Chkheidze 1989).

Figure 2. Two-dimensional diagram illustrating the arrangements of the seven transmembrane (TM) domains in visual opsins around the retinal chromophore (based on Bowmaker and Hunt 2006). Numbering of amino acid sites is based on bovine rhodopsin. Sites known to dictate spectral tuning are shown for each of the three visual pigments found in snakes, as well sites inferred to be under positive selection estimated by Bayes Empirical Bayes (model M8 β&ω). Sites inferred to be under positive selection associated with biochemical changes (detected by PRIME, SI Table S16-21) are marked with an asterisk (*). EL and CL are extra- and intracellular loops, respectively.

Figure 3. Spectral transmission curves for sampled snakes for (A) lenses and (B) spectacles, and (C) box-plots showing wavelength at which ocular media transmit 50% of the incident illumination (λ50%, top), and the proportion of UVA (315–400 nm) transmission (%UVA, bottom). The box plots summarise data for the lens (white), spectacle (grey) and lens + spectacle (black). Boxes extend from first (Q1) to third quartile (Q3); median is indicated as a horizontal line; whiskers extend to the observation that is closest to, but not more than, a distance of 1.5 (Q3 – Q1) from the

859 end of the box; outliers more distant than this are shown individually. All data newly
860 generated for this study except for *Pantherophis guttatus* (data from Thorpe 1991).

Supplementary Information

Table S1 . Identification and GenBank accession numbers of the samples used in this study.

Table S2. Ecological and retinal morphology classifications used in dN/dS analysis.

Table S3. Known amino acid spectral tuning sites for *rh1* opsin gene and predicted peak absorbance (λ_{max}) for snakes.

Table S4. Known amino acid spectral tuning sites for *sws1* opsin gene and predicted peak absorbance (λ_{max}) for snakes.

Table S5. Known amino acid spectral tuning sites for *lws* opsin gene and predicted peak absorbance (λ_{max}) for snakes.

Figure S6. *rh1* opsin gene phylogenetic tree under GTR+G+I model of sequence evolution.

Figure S7. *sws1* opsin gene phylogenetic tree under GTR+G+I model of sequence evolution.

Figure S8. *lws* opsin gene phylogenetic tree under GTR+G+I model of sequence evolution.

Figure S9. *rh1* opsin gene phylogenetic tree under GTR+G model of sequence evolution.

Figure S10. *sws1* opsin gene phylogenetic tree under GTR+G model of sequence evolution.

Figure S11. *lws* opsin gene phylogenetic tree under GTR+G model of sequence evolution.

Table S12. Ratio of synonymous to non-synonymous substitutions (dN/dS or ω) for snake visual opsin gene sequences under branch models.

Table S13. Ratio of synonymous to non-synonymous substitutions (dN/dS or ω) for snake visual opsin gene sequences under site models.

Table S14. Amino acid sites inferred as under positive selection (using Bayes Empirical Bayes), identified under site models in three visual opsin genes in snakes.

Table S15. Amino acid sites inferred as being under positive selection (using Bayes Empirical Bayes), identified under branch-site models for the three visual opsin genes in specific ecologies/lineages (foreground branch) in snakes.

Table S16. PRIME analysis for Atchley properties for the *sws1* opsin gene.

Table S17. PRIME analysis for Conant-Stadler properties for the *sws1* opsin gene.

Table S18. PRIME analysis for Atchley properties for the *lws* opsin gene.

Table S19. PRIME analysis for Conant-Stadler properties for the *lws* opsin gene.

Table S20. PRIME analysis for Atchley properties for the *rh1* opsin gene.

Table S21. PRIME analysis for Conant-Stadler properties for the *rh1* opsin gene.

Table S22. λ50% light cut-off and %UVA transmittance in lenses and spectacles in snakes.

Table S1. Identification and GenBank accession numbers of the samples used in this study.

Clade/Higher Taxon		Family	Species	Accession codes			
				16S	***rh1***	***sws1***	***lws***
Serpentes	Scolecophidia	Typhlopidae	*Amerotyphlops brongersmianus*	KR815889	KR336737	×	×
		Leptotyphlopidae	*Epictia collaris*	KR815892	KR336735	×	×
		Anomalepididae	*Liotyphlops beui*	KR815891	KR336734	×	×
		Anomalepididae	*Typhlophis squamosus*	KR815890	KR336733	×	×
	Alethinophidia	Aniliidae	*Anilius scytale*	KR815894	KR336736	×	×
		Tropidophiidae	*Tropidophis feicki*	KR815893	KR336738	KR336723	KR336709
		Xenopeltidae	*Xenopeltis unicolor*	NA	J49723	FJ497234	FJ497235
		Pythonidae	*Python regius*	NA	FJ497236	FJ4977237	FJ4977238
			Python bivittatus	NA		PRJNA238085	
		Boidae	*Gongylophis conicus*	xxxxxxxx	KX237870	KX237877	KX237782
		Uropeltidae	*Melanophidium khairei*	xxxxxxxx	KX237871	-	-
			Uropeltis cf. *macrolepis*	xxxxxxxx	KX237872	KX237878	KX237783
		Pareatidae	*Pareas monticola*	xxxxxxxx	KX237868	-	-
		Viperidae	*Bitis nasicornis*	xxxxxxxx	KX237873	KX237880	KX237785
			Echis ocellatus	xxxxxxxx	KX237874	KX237881	KX237786
			Causus rhombeatus	xxxxxxxx	KX237876	KX237882	KX237787
		Acrochordidae	*Acrochordus javanicus*	xxxxxxxx	KX237831	KX237879	KX237784
		Homolopsidae	*Enhydris innominata*	xxxxxxxx	KX237832	KX237883	KX237789
		Lamprophiidae	*Polemon collaris*	KR815896	KR336739	KR336724	KR336710
			Lamprophis olivaceus	xxxxxxxx	KX237859	KX237886	KX237827
			Malpolon monspessulanus	xxxxxxxx	×	KX237885	KX237790
			Lycophidion laterale	xxxxxxxx	KX237860	KX237887	KX237828
			Mehelya sp.	xxxxxxxx	KX237861	KX237888	KX237829
		Elapidae	*Ophiophagus hannah*	NA		PRJNA201683	

		Naja kaouthia	xxxxxxxx	KX237830	KX237884	KX237788
	Colubridae – Natricinae	*Amphiesma stolata*	xxxxxxxx	KX237866	KX237889	KX237792
		Xenochrophis piscator	xxxxxxxx	KX237865	KX237890	KX237801
		Natriciteres sylvatica	xxxxxxxx	KX237833	KX237891	KX237802
		Xylophis captaini	-	KX237869	KX237892	KX237791
		Natrix maura	KU323977	KU324002	KU323993	KU323982
		Thamnophis sirtalis	KU323978	KU323978	KU323994	KU323983
	Colubridae – Dipsadinae	*Atractus flammigerus*	KR815897	KR336740	KR336726	KR336712
		Atractus badius	xxxxxxxx	KX237842	KX237902	KX237809
		Heterodon nasicus	xxxxxxxx	KX237850	KX237893	KX237793
		Erythrolamprus reginae	xxxxxxxx	KX237855	KX237894	KX237800
		Helicops angulatus	xxxxxxxx	KX237836	KX237895	KX237806
		Thamnodynastes pallidus	xxxxxxxx	KX237864	KX237896	KX237805
		Xenopholis scalaris	xxxxxxxx	KX237834	KX237897	KX237810
		Pseudoboa coronata	xxxxxxxx	KX237837	KX237898	KX237803
		Oxyrhopus melanogenys	xxxxxxxx	KX237838	KX237899	KX237804
		Hypsiglena jani	KU323975	KU324007	KU323998	KU323988
		Imantodes lentiferus	xxxxxxxx	KX237841	KX237900	KX237807
		Leptodeira annulata	xxxxxxxx	KX237840	KX237901	KX237808
		Sibon nebulatus	xxxxxxxx	KX237843	KX237902	KX237811
		Dipsas indica	xxxxxxxx	KX237849	KX237904	KX237813
		Dipsas catesbyi	xxxxxxxx	KX237848	KX237905	KX237812
	Colubridae – Colubrinae	*Ahaetulla nasuta*	xxxxxxxx	KX237852	KX237906	KX237798
		Chrysopelea ornata	xxxxxxxx	KX237851	KX237907	KX237799
		Telescopus fallax	KU323974	KU324005	KU323995	KU323984
		Boiga forsteni	xxxxxxxx	KX237867	-	KX237818
		Boiga ceylonensis	xxxxxxxx	-	-	KX237819
		Dasypeltis scabra		KX237856	KX237908	KX237821
		Macroprotodon brevis	xxxxxxxx	--	KX237909	KX237815

			Spalerosophis diadema	xxxxxxxx	KX237853	KX237910	KX237814
			Hemorrhois hippocrepis	xxxxxxxx	KX237835	KX237911	KX237796
			Opheodrys aestivus	xxxxxxxx	KX237839	KX237912	KX237797
			Chironius fuscus	xxxxxxxx	KX237845	KX237913	KX237794
			Chironius carinatus	xxxxxxxx	KX237846	KX237914	KX237795
			Phyllorynchus decurtatus	KU323979	--	KU323996	KU323985
			Lycodon aulicus	xxxxxxxx	KX237875	KX237915	KX237820
			Orthriophis taeniurus	xxxxxxxx	KX237862	KX237916	KX237816
			Elaphe climacophora	xxxxxxxx	KX237845	KX237917	KX237817
			Pantherophis guttatus	xxxxxxxx	KX237863	KX237918	KX237824
			Pituophis catenifer	xxxxxxxx	KX237854	KX237919	KX237823
			Bogertophis subocularis	xxxxxxxx	KX237844	KX237920	KX237822
			Arizona elegans	KU323973	KU324006	KU323997	KU323986
			Lampropeltis californiae	xxxxxxxx	KX237858	KX237921	KX237825
			Lampropeltis floridiana	xxxxxxxx	KX237857	KX237922	KX237826
			Pseustes poecilonotus	KR815895	KR336741	KR336725	KR336711
Non-snake squamates	Lacertoidea	Amphisbaenidae	*Amphisbaena infraorbitale*	KR815886	KR336730	KR336719	KR336704
			Amphisbaena alba	KR815887	KR336729	KR336720	KR336705
			Amphisbaena sp.	KR815888	KR336728	KR336721	KR336706
		Lacertidae	*Takydromus sexlineatus*	KR815885	KR336727	KR336722	KR336707
		Gymnophthalmidae	*Bachia* cf. *flavescens*	KR815884	KR336731	KR336715	KR336703
	Scincoidea	Scincidae	*Melanoseps occidentalis*	KR815882	KR336743	KR336718	KR336713
		Scincidae	*Feylinia* sp.	KR815883	KR336742	KR336717	KR336714
	Anguimorpha	Diploglossidae	*Ophiodes striatus*	KR815881	KR336732	KR336716	KR336708
	Iguania	Dactyloidae	*Anolis carolinensis*	NA	Ensembl v75		
		Phrynosomatidae	*Uta stansburiana*	NA	DQ100323	DQ100325	DQ129869

Table S2. Ecology and retinal morphology classifications for sampled snakes. Y = yes, N = no, ? = not known, -- = inapplicable character. Cited references are generally not primary sources. The aim was to score as many cells as possible where 'reasonable' evidence was considered available. In some cases for retinal morphology we have extrapolated evidence from congeners. In a few cases we have extrapolated from information available for members of suprageneric taxa. Thus, uropeltid (*Melanophidium, Uropeltis*) retinal characters were scored based on data for the uropeltid *Rhinophis*; *Polemon* retinal characters were scored based on data for other atractaspidids; *Ophiophagus* and *Naja* scored for retinal characters based on data for other elapids.

Species	Primarily Fossorial	Primarily Arboreal	Aquatic or Semiaquatic	Primarily Diurnal	Double Cones Present	Transmuted Cones Present	Ecological source data	Retinal source data
Typhlophis squamosus	Y	N	N	N	--	--	Starace and Lambert 2013	Underwood 1967
Liotyphlops beui	Y	N	N	N	--	--	Kley 2003a	Underwood 1967
Epictia collaris	Y	N	N	N	--	--	Starace and Lambert 2013	Underwood 1967
Amerotyphlops brongersmianus	Y	N	N	N	--	--	Kley 2003b	Underwood 1967
Anilius scytale	Y	N	N	N	--	--	Starace and Lambert 2013	Underwood 1967
Tropidophis feicki	N	N	N	N	N	N	Schwartz 1957	Walls 1942; Underwood 1967
Xenopeltis unicolor	Y	N	N	N	N	N	Whitaker et al. 2004	Underwood 1967
Python bivittatus	N	N	N	N	N	N	Whitaker et al. 2004	Sillman et al. 1999
Python regius	N	N	N	N	N	N	www.toxinology.com	Sillman et al. 1999
Melanophidium khairei	Y	N	N	N	N	N	Gower et al. 2016	Baumeister 1908
Uropeltis cf. *macrolepis*	Y	N	N	N	N	N	Whitaker et al. 2004	Baumeister 1908
Gongylophis conicus	Y	N	N	N	N	N	Whitaker et al. 2004	Underwood 1967
Echis ocellatus	N	N	N	N	?	?	Chirio and LeBreton 2007	-
Causus rhombeatus	N	N	N	N	Y	N	Spawls et al. 2006	Underwood 1967
Bitis nasicornis	N	N	N	N	Y	N	Spawls et al. 2006	Walls 1942
Pareas monticola	N	Y	N	N	N	N	Ahmed et al. 2009	Underwood 1967, 1970
Acrochordus javanicus	N	N	Y	N	N	N	Das, 2015	Underwood 1967
Enhydris innominata	N	N	Y	N	Y	N	Murphy 2007	Underwood 1966
Polemon collaris	Y	N	N	N	?	N	Chirio and LeBreton 2007	Underwood 1967; Underwood & Kochva 1993
Lycophidion laterale	N	N	N	N	?	?	www.toxinology.com	-
Mehelya sp.	Y	N	N	N	?	?	Shine et al. 1996	-
Lamprophis olivaceus	N	N	N	N	Y	N	Spawls et al. 2006	Underwood 1967
Malpolon monspessulanus	N	N	N	Y	Y	N	Arnold and Ovenden 2002	Underwood 1967
Ophiophagus hannah	N	N	N	Y	Y	N	Ahmed et al. 2009	Underwood 1967, 1970
Naja kaouthia	N	N	N	Y	Y	N	www.thailandsnakes.com	Underwood 1967, 1970
Xenochrophis piscator	N	N	Y	Y	?	?	www.toxinology.com	-
Natriciteres sylvatica	N	N	Y	Y	?	?	www.toxinology.com	-
Amphiesma stolata	N	N	Y	Y	?	?	Whitaker et al. 2004	-
Natrix maura	N	N	Y	Y	Y	N	Arnold and Ovenden 2002	Underwood 1967
Thamnophis sirtalis	N	N	Y	Y	Y	N	Ernst and Ernst 2011	Sillman et al. 1997
Imantodes lentiferus	N	Y	N	N	?	?	Starace and Lambert 2013	-
Leptodeira annulata	N	Y	N	N	Y	Y	Starace and Lambert 2013	Underwood 1967, 1970
Atractus badius	Y	N	N	N	Y	N	Starace and Lambert 2013	Underwood 1970

Atractus flammigerus	Y	N	N	N	Y	N	Starace and Lambert 2013	Underwood 1970
Dipsas indica	N	Y	N	N	?	?	Starace and Lambert 2013	-
Dipsas catesbyi	N	Y	N	N	?	?	Starace and Lambert 2013	-
Sibon nebulatus	N	Y	N	N	Y	N	Starace and Lambert 2013	Underwood 1970
Hypsiglena jani	N	N	N	N	Y	Y	Starace and Lambert 2013	Walls 1942
Erythrolamprus reginae	N	N	Y	Y	?	?	Starace and Lambert 2013	-
Xenopholis scalaris	N	N	N	N	?	?	Starace and Lambert 2013	-
Pseudoboa coronata	N	N	N	N	Y	N	Starace and Lambert 2013	Underwood 1970
Oxyrhopus melanogenys	N	N	N	N	?	?	Starace and Lambert 2013	-
Helicops angulatus	N	N	Y	N	Y	N	Starace and Lambert 2013	Underwood 1970
Thamnodynastes pallidus	N	Y	N	N	?	?	Starace and Lambert 2013	-
Heterodon nasicus	N	N	N	Y	Y	N	Ernst and Ernst 2011	Underwood 1967
Ahaetulla nasuta	N	Y	N	Y	Y	N	Whitaker et al. 2004	Underwood 1967
Chrysopelea ornata	N	Y	N	Y	?	?	Whitaker et al. 2004	-
Telescopus fallax	N	N	N	N	Y	Y	Arnold and Ovenden 2002	Munk and Rasmussen 1993
Boiga forsteni	N	Y	N	N	Y	Y	Whitaker et al. 2004	Underwood 1967
Boiga ceylonensis	N	Y	N	N	Y	Y	Whitaker et al. 2004	Underwood 1967
Dasypeltis scabra	N	N	N	N	Y	Y	Spawls et al. 2006	Underwood 1967
Opheodrys aestivus	N	Y	N	Y	?	?	Ernst and Ernst 2011	-
Phyllorhynchus decurtatus	N	N	N	N	Y	Y	Ernst and Ernst 2011	Walls 1942
Pseustes poecilonotus	N	Y	N	Y	?	?	Starace and Lambert 2013	-
Chironius fuscus	N	Y	N	Y	?	?	Starace and Lambert 2013	-
Chironius carinatus	N	Y	N	Y	?	?	Starace and Lambert 2013	-
Lycodon aulicus	N	N	N	N	?	?	Whitaker et al. 2004	-
Orthriophis taeniurus	N	N	N	Y	?	?	www.toxinology.com	-
Elaphe climacophora	N	N	N	Y	?	?	www.toxinology.com	-
Pantherophis guttatus	N	N	N	N	?	?	Ernst and Ernst 2011	-
Pituophis catenifer	N	N	N	Y	?	?	Ernst and Ernst 2011	-
Arizona elegans	N	N	N	N	Y	Y	Ernst and Ernst 2011	Walls 1942
Lampropeltis californiae	N	N	N	Y	Y	Y	Ernst and Ernst 2011	Walls 1942
Lampropeltis floridiana	N	N	N	Y	Y	Y	Ernst and Ernst 2011	Walls 1942
Bogertophis subocularis	N	N	N	N	?	?	Ernst and Ernst 2011	-
Macroprotodon brevis	N	N	N	Y	?	?	www.afpmb.org	-
Spalerosophis diadema	N	N	N	Y	?	?	www.toxinology.com	-
Hemorrhois hippocrepis	N	N	N	Y	?	?	Arnold and Ovenden 2002	-
Xylophis captaini	Y	N	N	N	?	?	Gower and Winkler 2007	-

Table S3. Known amino acid spectral tuning sites for *rh1* (Yokoyama 2008; Hunt et al. 2001) and predicted peak absorbance (λ_{max}) of RH1-based visual pigment for snakes. Site values in first row represent amino acid positions numbered with respect to bovine rhodopsin. All λ_{max} values are predicted based on amino acid sequences (for a review see Yokoyama et al. 2008) except those in parentheses (measured using MSP or *in vitro* expression). When two mutations are present and the λ_{max} shift of the interaction is not known, the individual shift of each mutation is shown.

Species	**83**	**90**	**113**	**118**	**122**	**164**	**180**	**261**	**265**	**269**	**285**	**292**	**λ_{max} (nm)**
Bachia flavescens	**N**	G	E	T	E	A	P	F	W	A	P	A	491-496
Ophiodes striatus	**N**	G	E	T	E	A	P	F	W	A	P	A	491-496
Takydromus sexlineatus	**N**	G	E	T	E	A	P	F	W	A	P	A	491-496
Phelsuma madagascariensis	**N**	S	E	T	**Q**	A	P	F	W	A	**V**	A	-6|-20
Anolis carolinensis	**N**	G	E	T	E	A	P	F	W	A	P	A	491-496 (491[1])
Feylinia sp.	**N**	G	**K**	T	E	A	P	F	W	A	P	A	-6|?
Melanoseps occidentalis	**N**	G	E	T	E	A	P	F	W	A	P	A	491-496
Amphisbaena sp.	**N**	G	E	T	E	A	P	F	W	A	P	A	491-496
Amphisbaena alba	**N**	G	E	T	E	A	P	F	W	A	P	A	491-496
Amphisbaena infraorbitale	**N**	G	E	T	E	A	P	F	W	A	P	A	491-496
Amerotyphlops brongersmianus	**N**	G	E	T	E	A	P	F	W	A	P	A	491-496
Typhlophis squamosus	**N**	G	E	T	E	A	P	F	W	A	P	A	491-496
Liotyphops beui	**N**	G	E	T	E	A	P	F	W	A	P	A	491-496
Epictia collaris	**N**	G	E	T	E	A	P	F	W	A	P	A	491-496
Anilius scytale	**N**	G	E	T	E	A	P	F	W	A	P	A	491-496 (493[2])
Tropidophis feicki	**N**	G	E	T	E	A	P	F	W	A	P	A	491-496
Python regius	**N**	G	E	T	E	A	P	F	W	A	P	A	491-496 (494[3])
Python bivittatus	**N**	G	E	T	E	A	P	F	W	A	P	A	491-496
Xenopeltis unicolor	**N**	G	E	T	E	A	P	F	W	A	P	A	491-496 (499[4])
Gongylophis conicus	**N**	G	E	T	E	A	P	F	W	A	P	A	491-496
Melanophidium khairei	**N**	G	E	T	E	A	P	F	W	A	P	A	491-496
Uropeltis cf. *macrolepis*	**N**	G	E	T	E	A	P	F	W	A	P	A	491-496
Naja kaouthia	**N**	G	E	T	E	A	P	F	W	A	P	A	491-496
Ophiophagus hannah	**N**	G	E	T	E	A	P	F	W	A	P	**S**	476-489
Lamprophis olivaceus	D	G	E	T	E	A	P	F	W	A	P	A	500-505
Enhydris innominata	**N**	G	E	T	E	A	P	F	W	A	P	A	491-496
Acrochordus javanicus	**N**	G	E	T	E	A	P	F	W	A	P	A	491-496
Lycophidion laterale	**N**	G	E	T	E	A	P	F	W	A	P	A	491-496
Polemon collaris	**N**	G	E	T	E	A	P	F	W	A	P	**S**	476-489
Mehelya sp.	**N**	G	E	T	E	A	P	F	W	A	P	A	491-496

Species	83	90	113	118	122	164	180	261	265	269	285	292	λ_{max} (nm)
Pareas monticola	**N**	G	E	T	E	A	P	F	W	A	P	A	491-496
Xylophis captaini	**N**	G	E	T	E	A	P	F	W	A	P	**S**	476-489
Echis ocellatus	D	G	E	T	E	A	P	F	W	A	P	A	500-505
Bitis nasicornis	**N**	G	E	T	E	A	P	F	W	A	P	A	491-496
Causus rhombeatus	**N**	G	E	T	E	A	P	F	W	A	P	A	491-496
Natriciteres sylvatica	D	G	E	T	E	A	P	F	W	A	P	A	500-505
Thamnophis sirtalis	**N**	G	E	T	E	A	P	F	W	A	P	**S**	476-489 (482[5])
Natrix maura	**N**	G	E	T	E	A	P	F	W	A	P	**S**	476-489
Amphiesma stolata	**N**	G	E	T	E	A	P	F	W	A	P	**S**	476-489
Xenochrophis piscator	**N**	G	E	T	E	A	Q	F	W	A	P	**S**	476-489
Chrysopelea ornata	**N**	G	E	T	E	A	P	F	W	A	P	**S**	476-489
Ahaetulla nasuta	**N**	G	E	T	E	A	P	F	W	A	P	**S**	476-489
Spalerosophis diadema	**N**	G	E	T	E	A	P	F	W	A	P	**S**	476-489
Hemorrhois hippocrepis	**N**	G	E	T	E	A	P	F	W	A	P	**S**	476-489
Dasypeltis scabra	**N**	G	E	T	E	A	P	F	W	A	P	A	491-496
Telescopus fallax	D	G	E	T	E	A	P	F	W	A	P	A	500-505
Boiga forsteni	D	G	E	T	E	A	P	F	W	A	P	A	500-505
Ophoeodrys aestivus	**N**	G	E	T	E	A	P	F	W	A	P	**S**	476-489
Chironius carinatus	**N**	G	E	T	E	A	P	F	W	A	P	**S**	476-489
Chironius fuscus	**N**	G	E	T	E	A	P	F	W	A	P	**S**	476-489
Pseustes poecilonotus	**N**	G	E	T	E	A	P	F	W	A	P	**S**	476-489
Imantodes lentiferus	D	G	E	T	E	A	P	F	W	A	P	A	500-505
Hypsiglena jani	**N**	G	E	T	E	A	P	F	W	A	P	A	491-496
Leptodeira annulata	D	G	E	T	E	A	P	F	W	A	P	A	500-505
Atractus flammigerus	**N**	G	E	T	E	A	P	F	W	A	P	A	500-505
Atractus badius	**N**	G	E	T	E	A	P	F	W	A	P	**S**	476-489
Sibon nebulatus	D	G	E	T	E	A	P	F	W	A	P	A	500-505
Dipsas catesbyi	D	G	E	T	E	A	P	F	W	A	P	A	500-505
Dipsas indica	D	G	E	T	E	A	P	F	W	A	P	A	500-505
Helicops angulatus	**N**	G	E	T	E	A	P	F	W	A	P	A	491-496
Oxyrhopus melanogenys	D	G	E	T	E	A	P	F	W	A	P	A	500-505
Heterodon nasicus	**N**	G	E	T	E	A	P	F	W	A	P	**S**	476-489
Lycodon aulicus	**N**	G	E	T	E	A	P	F	W	A	P	A	491-496
Pseudoboa coronata	D	G	E	T	E	A	P	F	W	A	P	A	500-505
Xenopholis scalaris	**N**	G	E	T	E	A	P	F	W	A	P	A	491-496

Species	83	90	113	118	122	164	180	261	265	269	285	292	λ_{max} (nm)
Bogertophis subocularis	**N**	G	E	T	E	A	P	F	W	A	P	**S**	476-489
Elaphe climacophora	**N**	G	E	T	E	A	P	F	W	A	P	**S**	476-489
Pituophis catenifer	**N**	G	E	T	E	A	P	F	W	A	P	**S**	476-489
Erythrolampus reginae	**N**	G	E	T	E	A	P	F	W	A	P	**S**	476-489
Lampropeltis californiae	D	G	E	T	E	A	P	F	W	A	P	A	500-505
Lampropeltis floridiana	D	G	E	T	E	A	P	F	W	A	P	A	500-505
Arizona elegans	**N**	G	E	T	E	A	P	F	W	A	P	**S**	476-489 (484[6])
Orthriophis taeniurus	**N**	G	E	T	E	A	P	F	W	A	P	**S**	476-489
Pantherophis guttatus	**N**	G	E	T	E	A	P	F	W	A	P	A	491-496
Thamnodynastes pallidus	**N**	G	E	T	E	A	P	F	W	A	P	**S**	476-489
Ancestor Serpentes	**N**	G	E	T	E	A	P	F	W	A	P	A	491-496
Ancestor Alethinophidia	**N**	G	E	T	E	A	P	F	W	A	P	A	491-496
Ancestor Afrophidia	**N**	G	E	T	E	A	P	F	W	A	P	A	491-496
Ancestor Elapidae + Lamprophidae + Homolopsidae	**N**	G	E	T	E	A	P	F	W	A	P	A	491-496
Ancestor Viperidae	**N**	G	E	T	E	A	P	F	W	A	P	A	491-496
Ancestor Colubridae	**N**	G	E	T	E	A	P	F	W	A	P	**S**	476-489
Ancestor Colubrinae	**N**	G	E	T	E	A	P	F	W	A	P	**S**	476-489
Ancestor Natricinae	**N**	G	E	T	E	A	P	F	W	A	P	**S**	476-489
Ancestor Dipsadinae	**N**	G	E	T	E	A	P	F	W	A	P	**S**	476-489

[1]Yokoyama 2000; [2]Simões et al. 2015; [3]Davies et al. 2009; [4]Sillman et al. 1999; [5]Sillman et al. 1997; [6]Simões et al. 2016

Table S4. Known amino acid spectral tuning sites for *sws1* (Yokoyama et al. 2006) and predicted peak absorbance (λ_{max}) of SWS1-based visual pigment for snakes. Site values in first row represent amino acid positions numbered with respect to bovine opsin. Underline indicates amino acids with stronger effects on spectral tuning (Cowing et al. 2002; Babu et al. 2001; Asenjo et al. 1994 and Fasick et al. 2002). All λ_{max} values are predicted based on amino acid sequences (for a review see Yokoyama 2008) except those in parentheses (measured using MSP or *in vitro* expression). When two mutations are present and the λ_{max} shift of the interaction is unknown, the individual shift of each mutation is shown. An asterisk (*) marks a possible case of trichromacy. UVS = ultraviolet light sensitive (λmax c. 360nm).

Species	**46**	**49**	**52**	**86**	**90**	**93**	**97**	**113**	**114**	**116**	**118**	**265**	**λ_{max} (nm)**
Bachia flavescens	F	F	T	F	**S**	T	A	E	A	L	S	Y	UVS
Ophiodes striatus	A	F	T	F	**S**	T	A	E	A	L	S	Y	UVS
Takydromus sexlineatus	F	F	T	F	**S**	T	A	E	A	L	S	Y	UVS
Phelsuma madagascariensis	F	F	T	F	**S**	T	S	E	A	L	S	Y	UVS
Anolis carolinensis	F	F	T	F	**S**	T	A	E	A	L	S	Y	UVS (359[1])
Feylinia sp.	F	F	T	F	**S**	T	A	E	A	L	S	Y	UVS
Melanoseps occidentalis	F	F	T	F	**S**	T	A	E	A	L	S	Y	UVS
Amphisbaena sp.	F	F	T	F	**S**	T	A	E	A	L	S	Y	UVS
Amphisbaena alba	F	F	T	F	**S**	T	A	E	A	L	S	Y	UVS
Amphisbaena infraorbitale	F	F	T	F	**S**	T	A	E	A	L	S	Y	UVS
Tropidophis feicki	L	F	T	F	A	**A**	S	E	A	L	S	Y	UVS
Python regius	L	F	T	F	A	T	A	E	A	L	S	Y	UVS (361[2])
Python bivittatus	L	F	T	F	A	T	A	E	A	L	S	Y	UVS
Xenopeltis unicolor	L	F	T	F	A	T	A	E	A	L	S	Y	UVS (360[3])
Gongylophis conicus	L	F	T	F	A	T	A	E	A	L	S	Y	UVS
Uropeltis cf. *macrolepis*	L	F	T	F	**S**	T	A	E	A	L	S	Y	?
Naja kaouthia	L	F	T	F	A	**V**	S	E	A	L	**T**	Y	?
Ophiophagus hannah	L	F	T	F	A	**V**	S	E	A	L	**T**	Y	?
Lamprophis olivaceus	L	F	T	F	A	**V**	S	E	A	L	S	Y	?
Enhydris innominata	F	F	T	F	A	**V**	S	E	A	L	**T**	Y	?
Acrochordus javanicus	L	F	T	F	A	**V**	**C**	E	A	L	**T**	Y	?
Malpolon monspessulanus	L	L	T	**S**	A	**V**	T	E	A	L	S	Y	419|?
Polemon collaris	L	F	T	F	A	**V**	S	E	A	L	S	Y	?
Mehelya sp.	L	F	T	F	A	**V**	S	E	A	L	S	Y	?
Lycophidion laterale	L	F	T	F	A	**V**	S	E	A	L	S	Y	?

Species	46	49	52	86	90	93	97	113	114	116	118	265	λ_{max} (nm)
Xylophis captaini	L	F	T	F	A	T	S	E	A	L	S	Y	UVS
Echis ocellatus	L	F	T	F	A	**A**	S	E	A	L	S	Y	?
Bitis nasicornis	L	F	T	F	A	**A**	S	E	A	L	**T**	Y	?
Causus rhombeatus	L	C	T	F	A	T	S	E	A	**V**	S	Y	UVS
Natriciteres sylvatica	L	F	T	F	A	T	S	E	A	L	S	Y	UVS
Thamnophis sirtalis	L	F	T	F	A	T	S	E	A	L	S	Y	UVS (360[4])
Natrix maura	L	F	T	**L**	A	T	S	E	A	L	S	Y	UVS
Amphiesma stolata	L	F	T	F	A	**V**	S	E	A	L	**T**	Y	?
Xenochrophis piscator	L	F	T	F	A	**V**	S	E	A	L	**T**	Y	?
Chrysopelea ornata	L	F	T	**V**	A	**V**	S	E	A	L	**T**	Y	?
Ahaetulla nasuta	L	F	T	**V**	A	**V**	S	E	A	L	**T**	Y	?
Macroprotodon brevis	L	F	T	F	A	T	S	E	A	L	**T**	Y	UVS
Spalerosophis diadema	L	F	T	F	A	**V**	S	E	A	L	S	Y	?
Hemorrhois hippocrepis	L	F	T	F	A	**V**	S	E	A	L	S	Y	?
Dasypeltis scabra	L	F	T	F	A	**V**	S	E	A	L	**T**	Y	?
Telescopus fallax	L	F	T	F	A	**V**	**C**	E	A	L	**T**	Y	?
Ophoeodrys aestivus	L	F	T	F	A	**V**	S	E	A	L	**T**	Y	?
Chironius carinatus	L	F	T	**V**	A	**V**	S	E	A	L	**T**	Y	?
Chironius fuscus	L	F	T	**V**	A	**V**	S	E	A	L	**T**	Y	?
Pseustes poecilonotus	L	F	T	F	A	**V**	S	E	A	L	**T**	Y	?
Phyllorhynchus decurtatus	L	F	T	F	A	**V**	S	E	A	L	S	Y	?
Imantodes lentiferus	L	F	T	F	A	A	S	**D**	A	L	**T**	Y	-4|?
Hypsiglena jani	L	F	T	F	A	T	S	E	A	L	**T**	Y	UVS
Leptodeira annulata	L	F	T	F	A	T	S	E	A	L	**T**	Y	UVS
Atractus flammigerus	L	F	T	F	A	T	S	E	A	L	**T**	Y	UVS
Atractus badius	L	F	T	F	A	T	S	E	A	L	**T**	Y	UVS
Sibon nebulatus	L	F	T	F	A	T	S	E	A	L	**T**	Y	UVS
Dipsas catesbyi	L	F	T	F	A	T	S	E	A	L	**T**	Y	UVS
Dipsas indica	L	F	T	F	A	T	S	E	A	L	**T**	Y	UVS
Helicops angulatus	L	F	T	**VF**	A	**V**	S	E	A	L	**T**	Y	?*
Oxyrhopus melanogenys	L	F	T	F	A	**V**	S	E	A	L	**T**	Y	?
Heterodon nasicus	L	F	T	F	A	T	S	E	A	L	**T**	Y	UVS
Lycodon aulicus	L	F	T	F	A	**V**	S	E	A	L	**T**	Y	?
Pseudoboa coronata	L	F	T	F	A	**V**	S	E	A	L	**T**	Y	?
Xenopholis scalaris	L	F	T	F	A	T	S	E	A	L	**T**	Y	UVS

Species	**46**	**49**	**52**	**86**	**90**	**93**	**97**	**113**	**114**	**116**	**118**	**265**	**λ_{max} (nm)**
Bogertophis subocularis	L	F	T	F	A	**V**	S	E	A	L	S	Y	?
Elaphe climacophora	L	F	T	F	A	**V**	S	E	A	L	**T**	Y	?
Pituophis catenifer	L	F	T	F	A	**V**	S	E	A	L	S	Y	?
Erythrolampus reginae	L	F	T	F	A	T	S	E	A	L	**T**	Y	UVS
Lampropeltis californiae	L	F	T	F	A	**V**	S	E	A	L	**T**	Y	?
Lampropeltis floridiana	L	F	T	F	A	**V**	S	E	A	L	**T**	Y	?
Arizona elegans	L	F	T	F	A	**V**	S	E	A	L	**T**	Y	? (366[5])
Orthriophis taeniurus	L	F	T	F	A	**V**	S	E	A	L	**T**	Y	?
Pantherophis guttatus	L	L	T	**S**	A	**V**	T	E	A	L	S	Y	419|?
Thamnodynastes pallidus	L	F	T	F	A	**V**	S	E	A	L	S	Y	?
Ancestor Serpentes/ Alethiniphidia	L	F	T	F	A	A	S	E	A	L	S	Y	UVS
Ancestor Afrophidia	L	F	T	F	A	A	S	E	A	L	S	Y	UVS
Ancestor Elapidae + Lamprophidae + Homolopsidae	L	F	T	F	A	**V**	S	E	A	L	**T**	Y	UVS
Ancestor Viperidae	L	F	T	F	A	A	S	E	A	L	**T**	Y	UVS
Ancestor Colubridae	L	F	T	F	A	V	S	E	A	L	**T**	Y	UVS
Ancestor Colubrinae	L	F	T	F	A	V	S	E	A	L	**T**	Y	UVS
Ancestor Natricinae	L	F	T	F	A	T	S	E	A	L	**T**	Y	UVS
Ancestor Dipsadinae	L	F	T	F	A	T	S	E	A	L	**T**	Y	UVS

[1]Yokoyama 2000; [2]Davies et al. 2009; [3]Sillman et al. 1999; [4]Sillman et al. 1997; [5]Simões et al. 2016

Table S5. Known amino acid spectral tuning sites for *lws* (Yokoyama and Radlwimmer 1998) and predicted peak absorbance (λ_{max}) of LWS-based visual pigment for snakes. Site values in first row represent amino acid positions numbered with respect to bovine rhodopsin. Underline indicates amino acids with stronger effects on spectral tuning (Cowing et al. 2002; Babu et al. 2001; Asenjo et al. 1994 and Fasick et al. 2002). All λ_{max} values are predicted based on amino acid sequences (for a review see Yokoyama 2008) except those in parentheses (measured using MSP or *in vitro* expression).

Species	**180**	**197**	**277**	**285**	**308**	**λ_{max} (nm)**
Bachia flavescens	**A**	H	Y	T	A	555
Ophiodes striatus	S	H	Y	T	A	560
Takydromus sexlineatus	S	H	Y	T	A	560
Phelsuma madagascariensis	S	H	Y	T	A	560
Anolis carolinensis	S	H	Y	T	A	560 (560[1])
Feylinia sp.	**A**	H	Y	T	A	555
Melanoseps occidentalis	S	H	Y	T	A	560
Amphisbaena sp.	S	H	Y	T	A	560
Amphisbaena alba	S	H	Y	T	A	560
Amphisbaena infraorbitale	S	H	Y	T	A	560
Tropidophis feicki	**A**	H	Y	T	A	555
Python regius	S	H	Y	T	A	560 (551[2])
Python bivittatus	S	H	Y	T	A	560
Xenopeltis unicolor	S	H	Y	T	A	560 (558-562[3])
Gongylophis conicus	**A**	H	Y	T	A	555
Uropeltis cf. *macrolepis*	**A**	H	Y	T	A	555
Naja kaouthia	S	H	Y	T	A	560
Ophiophagus hannah	S	H	Y	T	A	560
Lamprophis olivaceus	**A**	H	Y	T	A	555
Enhydris innominata	S	H	Y	T	A	560
Acrochordus javanicus	S	H	Y	T	A	560
Malpolon monspessulanus	S	H	Y	T	A	560 (550-560[4])
Polemon collaris	S	H	Y	T	A	560
Mehelya sp.	**A**	H	Y	**A**	A	536
Lycophidion laterale	**A**	H	Y	T	A	555
Xylophis captaini	**A**	H	Y	T	A	555
Echis occelatus	**A**	H	Y	T	A	555
Bitis nasicornis	**A**	H	Y	T	A	555
Causus rhombeatus	**A**	H	Y	T	A	555
Natriciteres sylvatica	S	H	Y	T	A	560
Thamnophis sirtalis	**A**	H	Y	T	A	555 (553[5])
Natrix maura	**A**	H	Y	T	A	555
Amphiesma stolata	S	H	Y	T	A	560
Xenochrophis piscator	S	H	Y	T	A	560
Chrysopelea ornate	S	H	Y	T	A	560
Ahaetulla nasuta	S	H	Y	T	A	560
Spalerosophis diadema	**A**	H	Y	T	A	555
Hemorrhois hippocrepis	**A**	H	Y	T	A	560
Dasypeltis scabra	**A**	H	Y	**A**	A	536
Telescopus fallax	**A**	H	Y	**A**	A	536
Boiga forsteni	**A**	H	Y	**A**	A	536
Boiga ceylonensis	**A**	H	Y	**A**	A	536
Macroprotodon brevis	**A**	H	Y	T	A	555
Ophoeodrys aestivus	S	H	Y	T	A	560
Chironius carinatus	S	H	Y	T	A	560
Chironius fuscus	S	H	Y	T	A	560
Pseustes poecilonotus	S	H	Y	T	A	560

Species	**180**	**197**	**277**	**285**	**308**	**λ_{max} (nm)**
Phyllorhynchus decurtatus	**A**	H	Y	T	A	555
Imantodes lentiferus	**A**	H	Y	**A**	A	536
Hypsiglena jani	**A**	H	Y	**A**	A	536
Leptodeira annulata	**A**	H	Y	**A**	A	536
Atractus flammigerus	**A**	H	Y	**A**	A	536
Atractus badius	**A**	H	Y	**A**	A	536
Sibon nebulatus	**A**	H	Y	**A**	A	536
Dipsas catesbyi	**A**	H	Y	**A**	A	536
Dipsas indica	**A**	H	Y	**A**	A	536
Helicops angulatus	**A**	H	Y	T	A	555
Oxyrhopus melanogenys	**A**	H	Y	T	A	555
Heterodon nasicus	**A**	H	Y	**A**	**S**	?
Lycodon aulicus	**A**	H	Y	**A**	A	536
Pseudoboa coronata	**A**	H	Y	T	A	555
Xenopholis scalaris	**A**	H	Y	**A**	A	536
Bogertophis subocularis	**A**	H	Y	**A**	A	536
Elaphe climacophora	**A**	H	Y	T	A	555
Pituophis catenifer	**A**	H	Y	**A**	A	536
Erythrolampus reginae	S	H	Y	T	A	560
Lampropeltis californiae	**A**	H	Y	T	A	555
Lampropeltis floridiana	**A**	H	Y	T	A	555
Arizona elegans	**A**	H	Y	**A**	A	536 (538[6])
Orthriophis taeniurus	**A**	H	Y	T	A	555
Pantherophis guttatus	**A**	H	Y	**A**	A	536
Thamnodynastes pallidus	**A**	H	Y	T	A	555
Ancestor Serpentes/Alethiniphidia	**A**	H	Y	T	A	555
Ancestor Afrophidia	S	H	Y	T	A	560
Ancestor Elapidae + Lamprophidae + Homolopsidae	S	H	Y	T	A	560
Ancestor Viperidae	**A**	H	Y	T	A	555
Ancestor Colubridae	S	H	Y	T	A	560
Ancestor Colubrinae	S	H	Y	T	A	560
Ancestor Natricinae	S	H	Y	T	A	560
Ancestor Dipsadinae	**A**	H	Y	T	A	555

[1]Yokoyama 2000; [2]Sillman et al. 1999; [3]Davies et al. 2009; [4]Govardovskii & Chkheidze 1989; [5]Sillman et al. 1997; [6]Simões et al. 2016

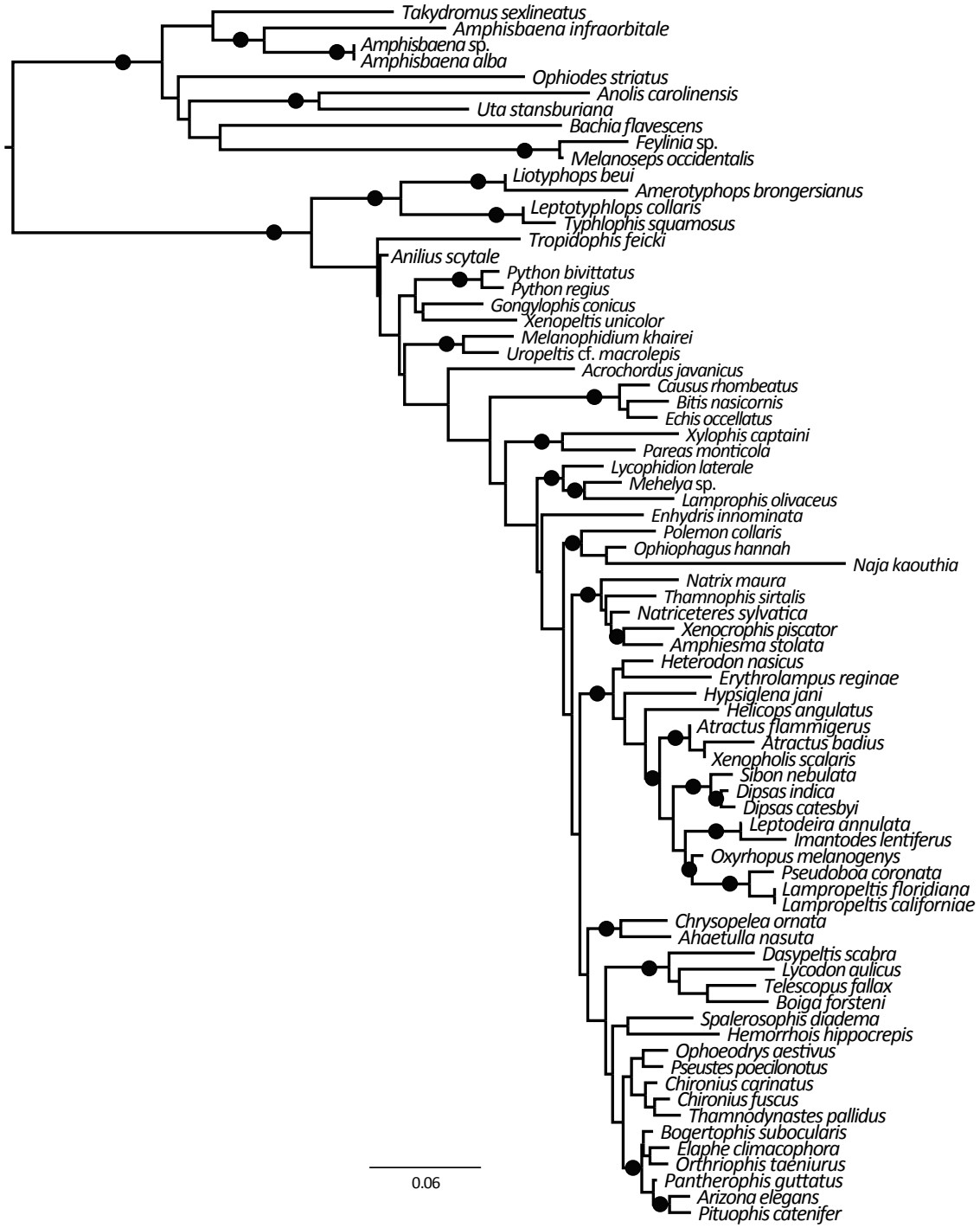

Figure S6. Maximum Likelihood rhodopsin 1 (*rh1*) gene phylogenetic tree for squamates estimated by RAxML based on GTR+G+I model of sequence evolution. Black circles in branches represent ML bootstrap support and Bayesian posterior probabilities above or equal to 80% and 1, respectively.

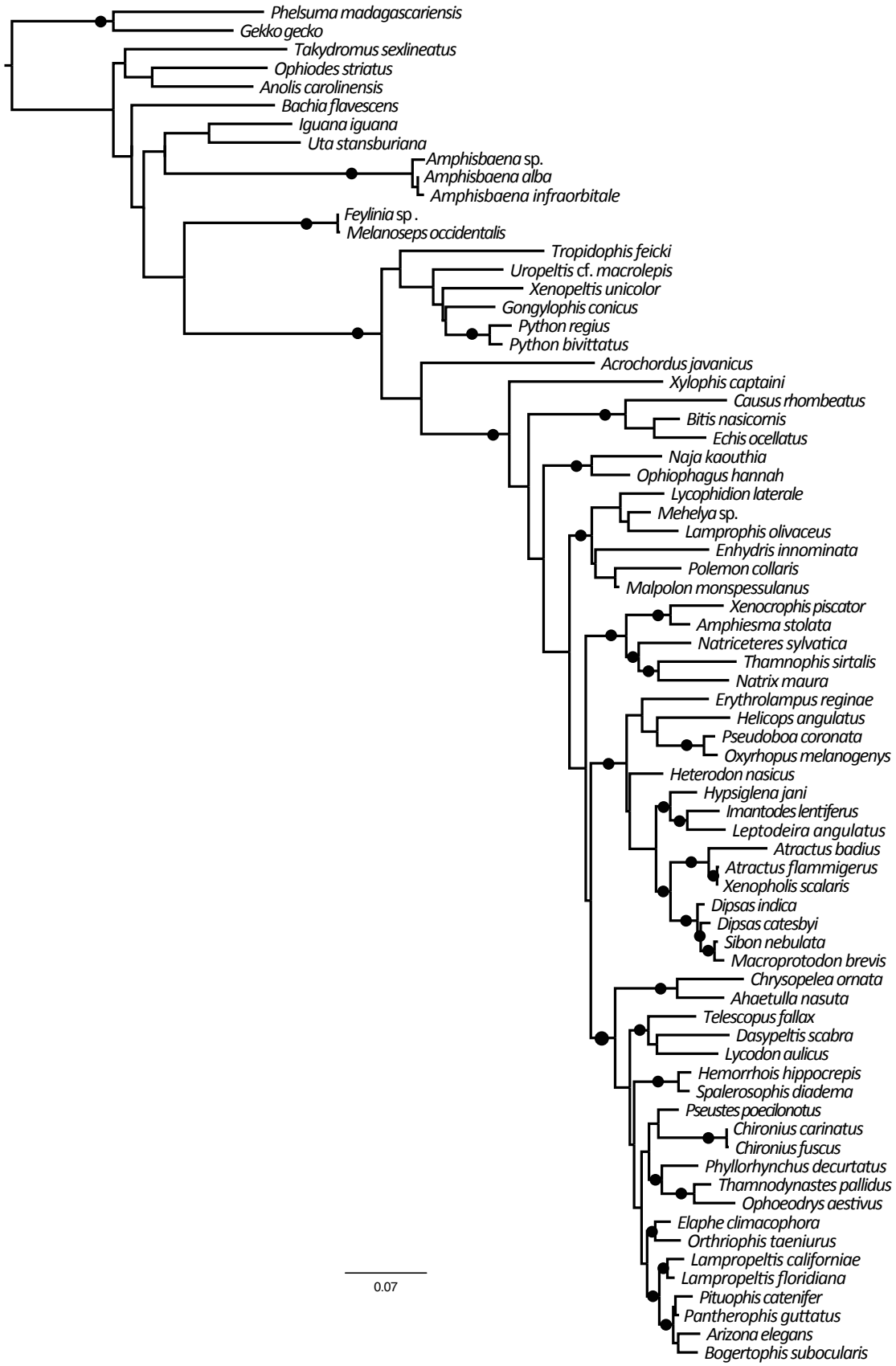

Figure S7. Maximum Likelihood short-wavelength opsin 1 (*sws1*) gene phylogenetic tree for squamates estimated by RAxML based on GTR+G+I model of sequence evolution. Black circles in branches represent ML bootstrap support and Bayesian posterior probabilities above or equal to 80% and 1, respectively.

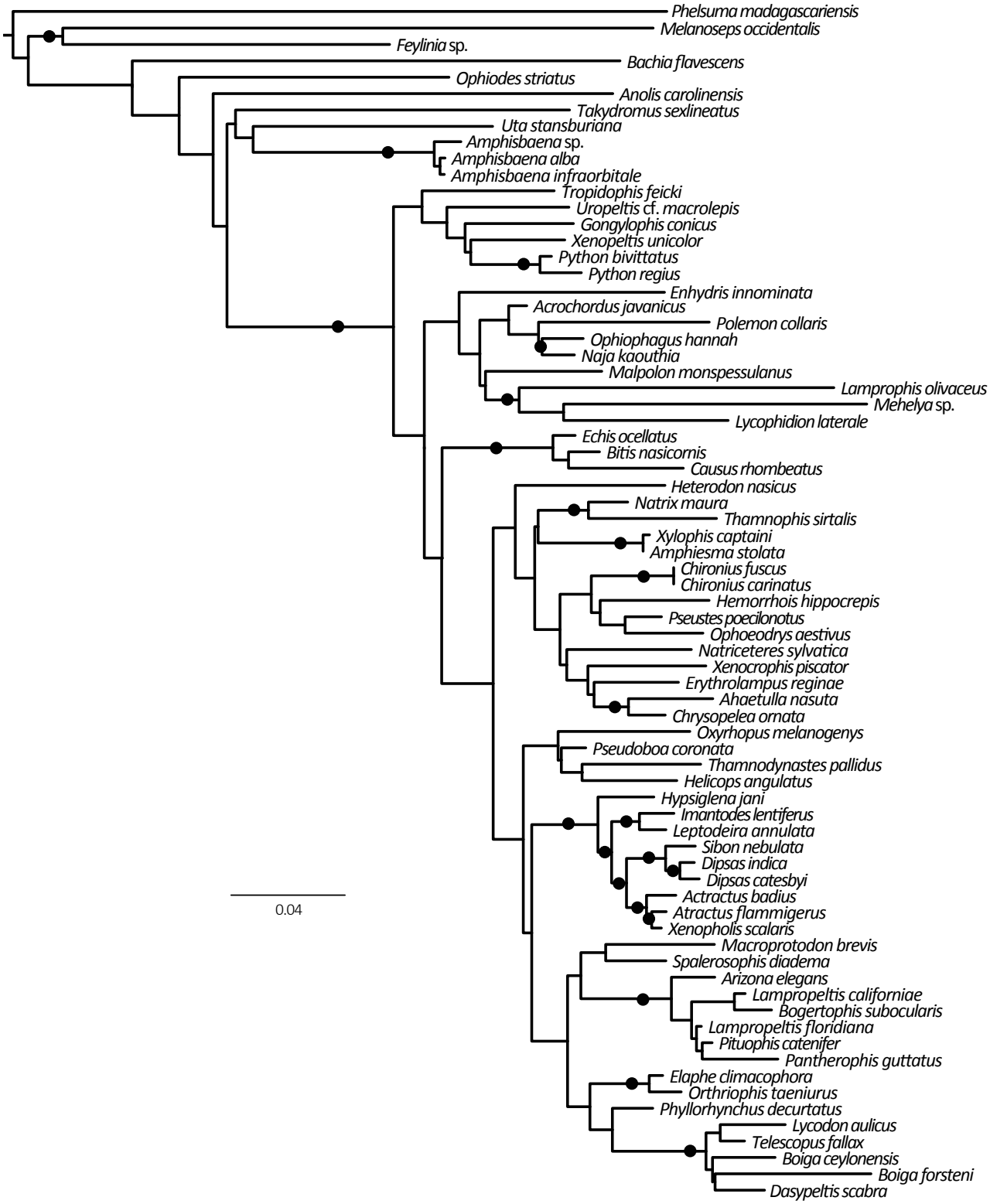

Figure S8. Maximum Likelihood medium-to-long wavelength opsin gene (*lws*) phylogenetic tree for squamates estimated by RAxML based on GTR+G+I model of sequence evolution. Numbers on the major internal branches are ML bootstrap support and Bayesian posterior probabilities, respectively.

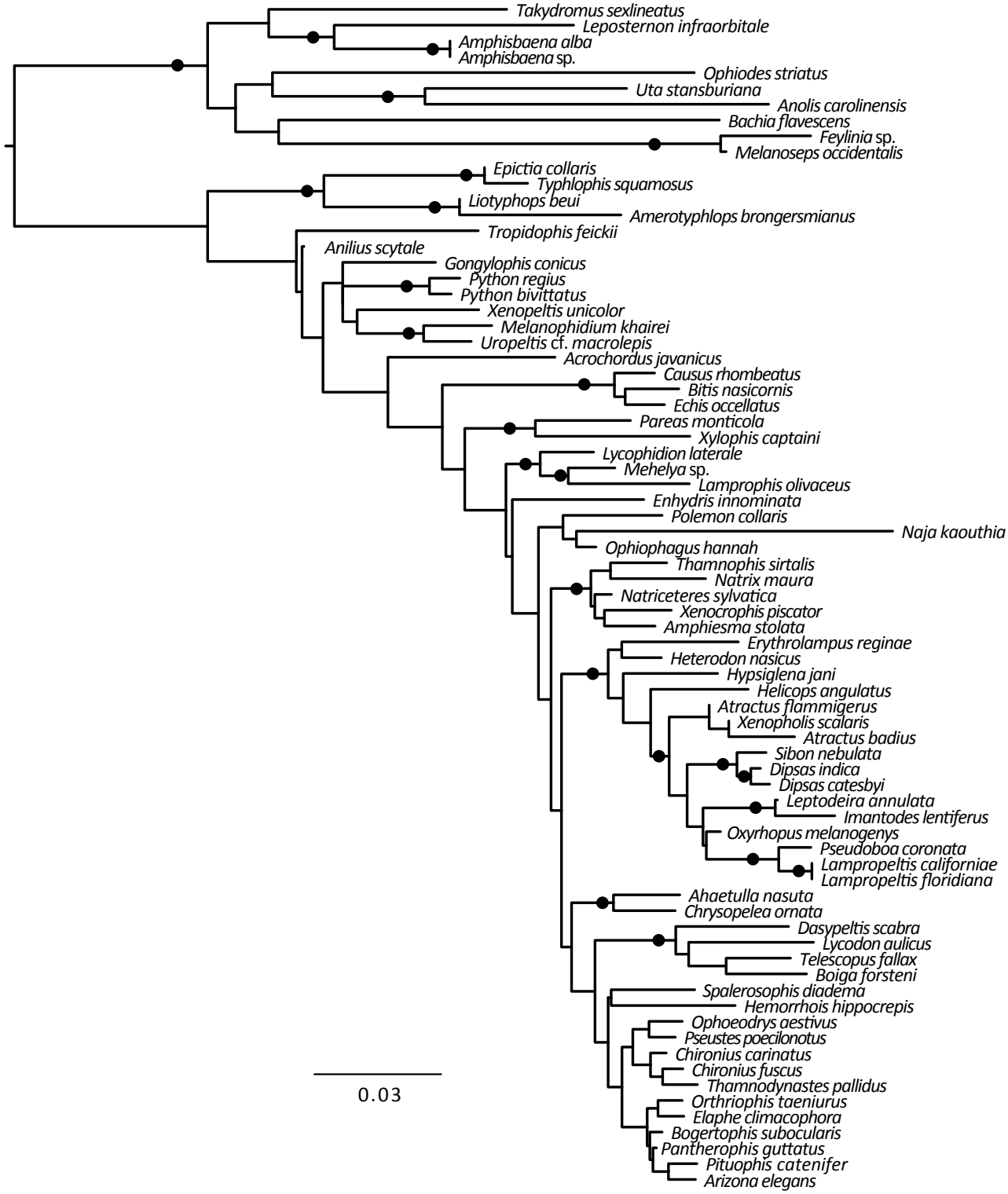

Figure S9. Maximum Likelihood rhodopsin 1 (*rh1*) gene phylogenetic tree for squamates estimated by RAxML based on GTR+G model of sequence evolution. Black circles in branches represent ML bootstrap support and Bayesian posterior probabilities above or equal to 80% and 1, respectively.

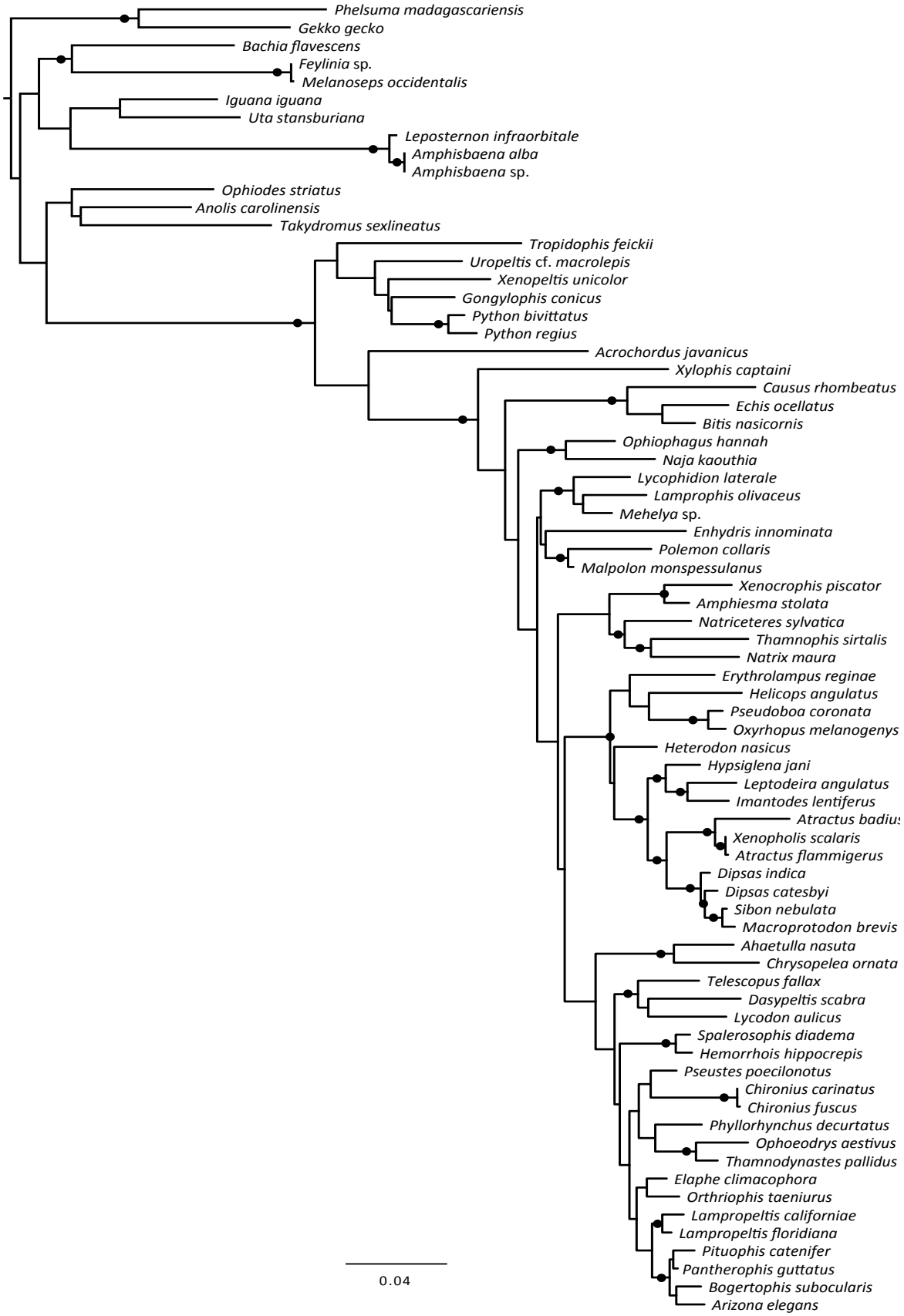

Figure S10. Maximum Likelihood short-wavelength opsin 1 (*sws1*) gene phylogenetic tree for squamates estimated by RAxML based on GTR+G model of sequence evolution. Black circles in branches represent ML bootstrap support and Bayesian posterior probabilities above or equal to 80% and 1, respectively.

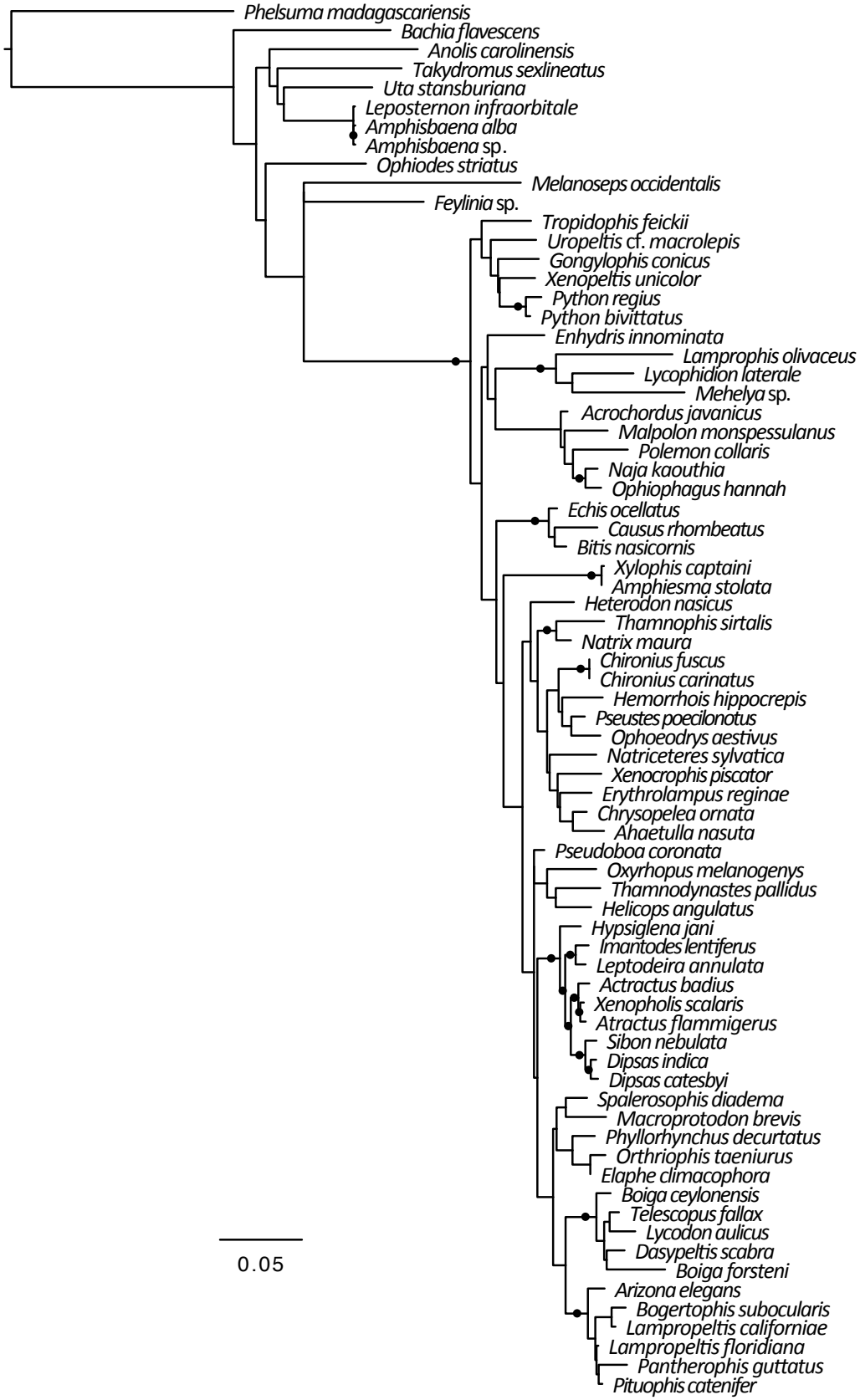

Figure S11. Maximum Likelihood medium-to-long wavelength opsin (*lws*) gene phylogenetic tree for squamates estimated by RAxML based on GTR+G model of sequence evolution. Black circles in branches represent ML bootstrap support and Bayesian posterior probabilities above or equal to 80% and 1, respectively.

Table S12. Ratio of synonymous to non-synonymous substitutions (dN/dS = ω) for snake visual opsin gene sequences under branch models. 2Δl = twice the difference logarithm of the likelihood value for the models; D.F. = degrees of freedom used to compare the models (corresponding with the number of free parameters).

Models	ω (d_N/d_S)	D.F.	Models Compared	2Δ (ln *L*)	P
1. *sws1* opsin gene					
A. All branches have one ω	ω= 0.107	-	-	-	-
B. Fossorial have ω_1; Non-fossorial ω_2	ω1= 0.062; ω2= 0.112	1	B vs. A	112.9	**2.3^{-26}**
C. Arboreal have ω_1; Non-arboreal ω_2	ω1= 0.097 ; ω2= 0.108	1	C vs. A	125.3	**4.4^{-29}**
D. (Semi)aquatic have ω_1; Non-aquatic ω_2	ω1= 0.092 ; ω2= 0.108	1	D vs. A	124.5	**6.7^{-29}**
E. Diurnal have ω_1; Nocturnal ω_2	ω1= 0.149 ; ω2= 0.099	1	E vs. A	117.9	**1.8^{-27}**
F. Colubrids have ω_1; Non-colubrids ω_2	ω1= 0.119; ω2= 0.088	1	F vs. A	117.4	**2.7^{-27}**
H. Every branch has it's own ω	Variable by branch	117	H vs. A	254.6	**3.5^{-12}**
1.1 *sws1* opsin gene (pruned)					
A1. All branches have one ω (double cones)	ω= 0.105	-	-	-	-
B1. All branches have one ω (transmuted)	ω= 0.105	-	-	-	-
C1. Double cone taxa have ω_1; others ω_2	ω1= 0.098; ω2= 0.110	1	C1 vs. A1	7.64	**0.002**
D1. Transmuted cone taxa have ω_1; others ω_2	ω1= 0.117; ω2= 0.101	1	D1 vs. B1	7.92	**0.004**
2. *lws* opsin gene					
I. All branches have one ω	ω= 0.312	-	-	-	-
J. Fossorial have ω_1; Non-fossorial ω_2	ω1= 0.116 ; ω2= 0.340	1	J vs. I	121.3	**3.4^{-28}**
K. Arboreal have ω_1; Non-arboreal ω_2	ω1= 0.398; ω2= 0.284	1	K vs. I	150.8	**1.1^{-34}**
L. (Semi)aquatic have ω_1; Non-aquatic ω_2	ω1= 0.268; ω2= 0.308	1	L vs. I	155.3	**1.2^{-35}**
M. Diurnal have ω_1; Nocturnal ω_2	ω1= 0.342; ω2= 0.296	1	M vs. I	155.3	**1.2^{-35}**
N. Colubrids have ω_1; Non-colubrids ω_2	ω1= 0.422; ω2= 0.193	1	N vs. I	105.5	**9.4^{-25}**
P. Every branch has it's own ω	Variable by branch	119	P vs. I	316.9	**6.5^{-20}**
2.1 *lws* opsin gene (pruned)					
I1. All branches have one ω (double cones)	ω= 0.311	-	-	-	-
J1. All branches have one ω (transmuted)	ω= 0.305	-	-	-	-
K1. Double cone taxa have ω_1; others ω_2	ω1= 0.387; ω2= 0.248	1	K1 vs. I1	66.18	**4.9^{-16}**
L1. Transmuted cone taxa have ω_1; others ω_2	ω1= 0.543; ω2= 0.273	1	L1 vs. J1	66.08	**4.3^{-16}**
3. *rh1* rhodopsin gene					
Q. All branches have one ω	ω= 0.237	-	-	-	-
R. Fossorial have ω_1; Non-fossorial ω_2	ω1= 0.161; ω2= 0.252	1	R vs. Q	183.7	**7.6^{-42}**
S. Arboreal have ω_1; Non-arboreal ω_2	ω1= 0.212; ω2= 0.240	1	S vs. Q	192.6	**8.7^{-44}**
T. (Semi)aquatic have ω_1; Non-aquatic ω_2	ω1= 0.253; ω2= 0.229	1	T vs. Q	193.2	**6.4^{-44}**
U. Diurnal have ω_1; Nocturnal ω_2	ω1= 0.141; ω2= 0.240	1	U vs. Q	188.4	**7.2^{-43}**
V. Colubrids have ω_1; Non-colubrids ω_2	ω1= 0.252; ω2= 0.212	1	V vs. Q	191.0	**1.9^{-43}**
W. Scolecophidia have ω_1; Alethinophidia ω_2	ω1= 0.141; ω2= 0.244	1	W vs. Q	193.2	**6.4^{-44}**
Y. Every branch has its own ω	Variable by branch	127	Y vs. Q	272.2	**1.4^{-12}**
3.1 *rh1* rhodopsin gene (pruned)					
Q1. All branches have one ω (double cones)	ω= 0.244	-	-	-	-
R1. All branches have one ω (transmuted)	ω=0.245	-	-	-	-
S1. Double cone taxa have ω_1; others ω_2	ω1= 0.295; ω2= 0.189	1	S1 vs. Q1	68.22	**5.7^{-15}**
T1. Transmuted cone taxa have ω_1; others ω_2	ω1= 0.388; ω2= 0.212	1	T1 vs. R1	65.23	**6.7^{-16}**

Tabl S13. Ratio of synonymous to non-synonymous substitutions (dN/dS = ω) for snake visual opsin gene sequences under site models. For each gene two pairs of models are compared to test for significant difference in goodness-of-fit to data. 2Δl = twice the difference logarithm of the likelihood value for the models; D.F. = degrees of freedom used to compare the models (corresponding with the number of free parameters).

Models	Parameters	D.F.	Models Compared	2Δ (ln *L*)	P
1. *sws1* opsin gene					
A. M1a	ω0 = 0.039, ω1 = 1, *p0* = 0.829 (*p1* = 0.171)	-	-	-	-
B. M2a	ω0 = 0.039, ω1 = 1, ω2 = 4.230, *p0* = 0.830, *p1* = 0.168 (*p*2 = 0.002)	2	B vs. A	34.36	**3.4^{-8}**
C. M7	*p* = 0.154, *q* = 0.858	-	-	-	**-**
D. M8 (β&ω)	*p0* = 0.997 (*p1* = 0.003), *p*= 0.158, *q* = 0.923, ω_S = 3.501	2	D vs. C	24	**6.1^{-6}**
2. *lws* opsin gene					
E. M1a	ω0 = 0.032, ω1 = 1, *p0* = 0.807 (*p1* = 0.193)	-	-	-	-
F. M2a	ω0= 0.036, ω1= 1, ω2= 3.037, *p0* = 0.800, *p1* = 0.140 (*p*2 =0.059)	2	F vs. E	152.5	**7.8^{-34}**
G. M7	*p* = 0.085, *q* = 0.317	-	-	-	**-**
H. M8 (β&ω)	*p0* = 0.927 (*p1* = 0.073), *p* = 0.111, *q* = 0.602, ω_S = 0.693	2	H vs. G	153.3	**5.2^{-34}**
2. *rh1* hodopsin 1 gene					
I. M1a	ω0 = 0.032, ω1 = 1, *p0* = 0.789 (*p1* = 0.211)	-	-	-	-
J. M2a	ω0 = 0.033, ω1 = 1, ω2 = 2.46, *p0* = 0.786, *p1* = 0.182 (*p*2 = 0.032)	2	J vs. I	29.9	**3.2^{-7}**
K. M7	*p* = 0.103, *q* = 0.408	-	-	-	**-**
L. M8 (β&ω)	*p0* = 0.935 (*p1* = 0.065), *p* = 0.144, *q* = 0.925, ω_S = 1.881	2	L vs. K	42.22	**6.8^{-10}**

Table S14. Amino acid sites inferred to be under positive selection (using Bayes Empirical Bayes), identified under site models for the three visual opsin genes in snakes. Sites in bold are those known to be associated with spectral tuning of the corresponding visual pigment and those marked with an asterisk are associated with stabilization of the chromophore (retinal) pocket.

Models	Sites Under Positive Selection
1. *sws1* opsin gene	
B. M2a	13 – 152
D. M8 (β&ω)	**86** – **93** – 103 – 106 – 110 – 120 – 257
2. *lws* opsin gene	
F. M2a	55 – 61 – 120 – 128* - 140 – 170 – 174 – **180** – 181 – 229 – 234 – 305
H. M8 (β&ω)	55 – 61 – 65 – 128* – 135 – 140 – 170 – 174 – **180** – 181 – 221 – 224* – 229 – 234 – **285** – 286 – 292 – 305
2. *rh1* rhodopsin gene	
J. M2a	19 – 81 – **83** – 112 – 119* – 133 – 159 – 213 – 217 – 290 - 299
L. M8 (β&ω)	11 – 19 – 81 – **83** – 112 – 119* – 133 – 158 – 159 – 173 – 209* – 213 – 217 – 290 – **292** – 299

Table S15. Amino acid sites inferred to be under positive selection (using Bayes Empirical Bayes), identified under branch-site models for the three visual opsin genes in particular phenotypic or phylogenetic groups (foreground branch) in snakes. Sites in bold are those known to be associated with spectral tuning.

Gene	Foreground branch	Sites under positive selection	2Δl	P Value
lws	Colubridae	24 – 28 – 54 – 119 – 127 – 169 – **180** – 181 – 214 – 220 – 229 – 234 – **285** – 305	107.1	5.5^{-24}
	Aquatic	181 – 229	16.88	0.0002
	Arboreal	31 – 130 – 131 – 198 – 239 – 297	47.88	4.0^{-11}
	Fossorial	None	16.76	0.0002
	Diurnal	54 – 127 – **180** – 181 – 229 – 291 – 305	81.42	2.0^{-18}
sws1	Colubridae	207 – 257 – 280 – 327	20.9	2.89^{-05}
	Aquatic	141	36.68	1.08^{-08}
	Arboreal	98 – 176 – 197	30.34	2.58^{-07}
	Fossorial	50 – 61	25.08	3.58^{-06}
	Diurnal	84 – 98 – 107	27.32	1.16^{-06}
rh1	Colubridae	155 – 213	8.4	0.0145
	Aquatic	48 – 155	8.6	0.0136
	Arboreal	30 – 217 – 323 – 332	6.92	0.0314
	Fossorial	168 – 210 – 241	7.52	0.0233
	Diurnal	4 – 38 – 151 – 155	13.08	0.0014

Table S16. Sites with changing properties under PRIME analysis for Atchley properties for the *sws1* opsin gene. Changing properties are marked in bold.

Codon	t	α1	p1	α2	p2	α3	p3	α4	p4	α5	p5
28	1.944	0.840	1.000	2.159	0.824	15.938	0.080	8.291	0.879	**-13.97**	**0.018**
40	0.259	3.683	0.211	**-2.59**	**0.011**	0.368	1.000	-0.075	1.000	-0.888	0.812
51	0.956	0.855	0.513	0.594	0.755	-0.920	1.000	**-6.268**	**0.008**	7.687	0.688
84	0.008	2.414	0.057	-1.195	1.000	1.250	0.875	**-4.338**	**0.031**	-0.815	0.175
107	0.160	1.172	1.000	18.280	0.410	-0.617	1.000	**-4.653**	**0.036**	-0.086	1.000
177	1.283	1.992	0.518	16.784	0.325	**-5.560**	**0.043**	12.932	0.026	0.508	0.446
211	0.078	2.106	0.080	12.148	0.031	**-4.740**	**0.000**	5.059	0.005	1.416	0.015
222	1.937	6.047	0.000	-0.874	0.192	0.107	1.000	**-1.684**	**0.031**	0.653	0.601
313	0.340	11.350	0.068	**-2.392**	**0.000**	0.086	1.000	1.258	1.000	-0.023	1.000
331	5.181	3.327	0.019	**-1.538**	**0.032**	-0.016	1.000	6.020	0.017	-0.352	0.246

Table S17. Sites with changing properties under PRIME analysis for Conant-Stadler properties for the *sws1* opsin gene. Changing properties are marked in bold.

Codon	t	α1	p1	α2	p2	α3	p3	α4	p4	α5	p5
11	0.317	-1.559	1.000	-1.323	1.000	16.937	1.000	0.968	1.000	**-3.556**	**0.003**
13	0.065	-1.387	1.000	-1.894	1.000	20.000	1.000	0.547	1.000	**-5.047**	**0.039**
54	0.218	**-2.416**	**0.035**	-0.119	1.000	0.074	1.000	14.246	0.335	-0.319	1.000
79	1.127	20.000	0.037	0.300	0.940	0.143	1.000	**-20.00**	**0.012**	14.148	0.037
103	1.661	20.000	0.075	1.297	1.000	-0.048	1.000	**-20.00**	**0.008**	14.660	0.027
120	0.526	20.000	0.001	**-12.97**	**0.006**	11.032	0.007	1.029	0.033	-2.232	0.155
313	0.636	**-2.724**	**0.003**	0.497	0.785	0.377	1.000	20.000	0.000	0.493	1.000
331	3.727	**-3.055**	**0.028**	2.709	0.038	**-1.280**	**0.034**	19.245	0.023	1.076	1.000

Table S18. Sites with changing properties under PRIME analysis for Atchley properties for the *lws* opsin gene. Changing properties are marked in bold.

Codon	t	α1	p1	α2	p2	α3	p3	α4	p4	α5	p5
17	13.425	3.179	1.000	1.524	0.016	2.227	0.002	0.058	1.000	**-2.744**	**0.002**
54	1.584	3.743	0.004	-1.881	0.128	**-2.216**	**0.001**	**-3.667**	**0.010**	9.560	0.000
140	2.181	6.755	0.049	**-2.706**	**0.002**	1.363	1.000	1.265	1.000	0.393	1.000
176	0.002	5.478	0.554	**-3.017**	**0.026**	-0.316	1.000	-0.239	1.000	-0.008	0.966
180	0.082	8.744	0.638	**-1.886**	**0.009**	-0.587	1.000	-0.966	1.000	0.328	1.000
181	3.057	6.106	0.000	-0.479	0.128	0.577	0.080	**-3.543**	**0.002**	-0.637	0.139
225	0.494	0.584	1.000	**-2.122**	**0.013**	0.194	0.511	0.195	0.836	-0.261	1.000
230	1.173	1.364	0.019	0.313	0.473	1.254	0.019	0.306	1.000	**-2.402**	**0.004**

Table S19. Sites with changing properties under PRIME analysis for Conant-Stadler properties for the *lws* opsin gene. Changing properties are marked in bold.

Codon	t	α1	p1	α2	p2	α3	p3	α4	p4	α5	p5
132	3.155	0.268	0.481	**-9.982**	**0.008**	0.605	0.573	10.505	0.031	7.309	0.008
168	1.779	20.000	0.024	**-20.00**	**0.007**	16.512	0.090	15.514	0.061	1.236	0.464
181	2.422	0.556	0.253	**-9.902**	**0.000**	12.121	0.000	19.883	0.000	-0.876	0.327
245	3.728	20.000	0.000	**-19.09**	**0.000**	17.237	0.000	11.033	0.000	0.649	0.750

Table S20. . Sites with changing properties under PRIME analysis for Atchley properties for the *rh1* opsin gene. Changing properties are marked in bold.

Codon	t	α1	p1	α2	p2	α3	p3	α4	p4	α5	p5
4	1.629	-1.441	0.096	20.000	0.103	-0.281	1.000	**-13.85**	**0.017**	2.576	0.067
19	0.444	1.232	1.000	2.110	0.937	1.314	0.401	-0.308	0.935	**-3.16**	**0.019**
30	0.499	0.933	1.000	-1.202	1.000	0.872	1.000	**-4.807**	**0.017**	0.481	1.000
57	0.872	19.500	0.788	1.952	0.591	0.764	0.494	**-7.650**	**0.000**	0.417	0.445
154	0.474	1.301	0.274	0.536	1.000	-0.732	0.246	**-2.963**	**0.007**	2.201	0.076
214	2.458	0.095	1.000	-0.059	1.000	2.288	0.012	1.290	0.748	**-2.697**	**0.041**
232	0.033	0.966	1.000	-0.324	1.000	**-3.532**	**0.045**	0.796	1.000	9.781	0.005
248	0.520	5.908	0.063	1.156	1.000	-1.086	1.000	**-5.570**	**0.016**	0.678	0.672
308	0.880	1.312	1.000	-0.742	1.000	**-2.456**	**0.005**	1.340	0.539	3.680	0.032
318	0.619	1.587	1.000	1.296	1.000	**-3.349**	**0.022**	0.246	1.000	5.352	0.059
332	0.861	**-6.025**	**0.048**	-0.692	1.000	0.232	1.000	10.358	0.010	0.067	1.000

Table S21. Sites with changing properties under PRIME analysis for Conant-Stadler properties for the *rh1* opsin gene. Changing properties are marked in bold.

Codon	t	α1	p1	α2	p2	α3	p3	α4	p4	α5	p5
41	0.504	**-4.465**	**0.006**	0.418	0.232	-2.915	0.054	20.000	0.022	5.871	0.033
57	0.675	20.000	1.000	0.665	0.736	10.604	0.591	3.646	1.000	**-8.104**	**0.008**
169	0.634	-1.819	0.365	0.937	1.000	-0.111	1.000	**20.000**	**0.001**	-0.572	1.000
185	0.774	-1.423	0.572	**-11.56**	**0.034**	4.003	0.644	-1.957	0.598	14.370	0.040
217	7.231	3.924	0.562	**-3.880**	**0.024**	0.694	0.750	4.338	0.000	-0.419	1.000
270	0.474	20.000	0.210	**-20.00**	**0.008**	11.823	0.066	14.749	0.055	0.665	1.000

Table S22. λ50% light cut-off and %UVA transmission in lenses and spectacles in snakes. All data newly generated for this study except for *Pantherophis guttatus* (data from Thorpe 1991).

Family	Species (number of lenses, spectacles)	Mean Lens Diameter (mm)	%UVA		Total %UVA	λ50% (nm)	
			Lens	Spectacle		Lens	Spectacle
Acrochordidae	*Acrochordus javanicus* (1,2)	1.35	97.4	52.8	51.2	310	346
Homolopsidae	*Enhydris innominata* (2,2)	—	68.1	49.6	34.8	324	355
Lamprophiidae	*Malpolon monspessulanus* (2,0)	2.13	1.7	—	—	451	—
	Lamprophis olivaceus (1,0)	1.35	87.2	—	—	306	—
Elapidae	*Naja kaouthia* (2,2)	1.95	80.4	47.7	38.8	312	360
Colubridae	*Thamnophis sirtalis* (1,1)	1.75	35.8	61.8	21.6	413	340
	Ahaetulla nasuta (2,0)	1.75	7.6	—	—	424	—
	Chrysopelea ornata (2,2)	2.75	1.9	33.9	0.4	438	371
	Telescopus fallax (2,2)	1.58	39.3	74.3	29.5	380	304
	Opheodrys aestivus (2,2)	1.63	37.8	48.5	18.9	398	354
	Spalerosophis diadema (2,2)	2.33	21.3	63.5	13.5	417	338
	Elaphe climacophora (2,2)	1.87	51.2	58.6	31.5	357	346
	Pituophis catenifer (1,2)	2.15	46.2	45.7	23.3	373	355
	Orthriophis taeniurus (2,2)	2.01	57.0	56.5	34.1	327	348
	Bogertophis subocularis (2,2)	1.95	93.2	58.3	55.9	313	345
	Dasypeltis scabra (1,2)	2.20	66.2	74.5	49.4	318	315
	Arizona elegans (2,2)	2.10	63.0	73.5	48.0	327	330
	Heterodon nasicus (1,2)	—	—	40.6	—	—	368
	Pantherophis guttatus (1,0)	2.89	28.2	—	—	385	—

References

Ahmed MF, Das A, Dutta SK. 2009. Amphibians and Reptiles of Northeast India. Aaranyak: Guwahati

Arnold N, Ovenden D. 2002. A Field Guide to the Reptiles and Amphibians of Britain and Europe. HarperCollins UK

Asenjo AB, Rim J, Oprian DD. 1994. Molecular determinants of human red/green color discrimination. Neuron 12:1131–1138.

Babu KR, Dukkipati A, Birge RR, Knox BE. 2001. Regulation of Phototransduction in Short-Wavelength Cone Visual Pigments via the Retinylidene Schiff Base Counterion. Biochemistry 40:13760–13766.

Baumeister L. 1908. Beiträge zur anatomie und physiologie der Rhinophiden. Integument, Drüsen der Mundhöhle, Augen und Skeletsystem. :423–526.

Chirio L, LeBreton M. 2007. Atlas des reptiles du Cameroun. IRD Editions

Cowing JA, Poopalasundaram S, Wilkie SE, Robinson PR, Bowmaker JK, Hunt DM. 2002. The molecular mechanism for the spectral shifts between vertebrate ultraviolet- and violet-sensitive cone visual pigments. Biochem. J. 367:129.

Das, I. 2015. A Field Guide To The Reptiles Of South-East Asia. London: Bloomsbury Publishing.

Davies WL, Cowing JA, Bowmaker JK, Carvalho LS, Gower DJ, Hunt DM. 2009. Shedding Light on Serpent Sight: The Visual Pigments of Henophidian Snakes. J. Neurosci. 29:7519–7525.

Ernst CH, Ernst EM. 2011. Venomous Reptiles of the United States, Canada, and Northern Mexico. JHU Press

Fasick JI, Applebury ML, Oprian DD. 2002. Spectral tuning in the mammalian short-wavelength sensitive cone pigments. Biochemistry 41:6860–6865.

Govardovskii VI, & Chkheidze NI (1989). Retinal photoreceptors and visual pigments in certain snakes. Biological Abstracts, 90: 1036.

Gower DJ, Giri V, Captain A, Wilkinson M. 2016. A reassessment of *Melanophidium* Günther, 1864 (Reptilia: Serpentes: Uropeltidae) from the Western Ghats of peninsular India, with the description of a new species. Zootaxa 4085: 481–503.

Gower DJ, Winkler JD. 2007. Taxonomy of the Indian snake Xylophis Beddome (Serpentes: Caenophidia), with description of a new species. Hamadryad 31:315–329.

Hunt DM, Dulai KS, Partridge JC, Cottrill P, Bowmaker JK. 2001. The molecular basis for spectral tuning of rod visual pigments in deep-sea fish. J. Exp. Biol. 204:3333–3344.

Kley NJ. 2003a. Early blindsnakes (Anomalepididae). In: Hitchins M, Murphy JB, Schlager N, editors. Grzimeks Animal Life Encyclopedia. Vol. 7. Farmington Hills, MI. pp. 369–372.

Kley NJ. 2003b. Blindsnakes (Typhlopidae). In: Hutchins M, Murphy JB, Schlager N, editors. Grzimeks Animal Life Encyclopedia. Vol. 7. Farmington Hills, MI: Gale Group. pp. 379–385.

Munk O, Rasmussen JB. 1993. Note on the Rod-like Photoreceptors in the Retina of the Snake *Telescopus fallax* (Fleischmann, 1831). Acta Zool. 74:9–13.

Murphy JC. 2007. Homalopsid Snakes. Malabar, Florida: Krieger Publishing Company

Schwartz A. 1957. A new species of boa (genus Tropidophis) from western Cuba. American Museum Novitates: 8.

Shine R, Branch WR, Harlow PS, Webb JK. 1996. Sexual dimorphism, reproductive biology, and food habits of two species of African filesnakes (Mehelya, Colubridae). J. Zool. Lond. 240:327–340.

Sillman AJ, Carver JK, Loew ER. 1999. The Photoreceptors and Visual Pigments in the Retina of a Boid Snake, the Ball Python (*Python regius*). J. Exp. Biol. 202:1931–1938.

Sillman AJ, Govardovskii VI, Rohlich P, Southard JA, Loew ER. 1997. The photoreceptors and visual pigments of the garter snake (Thamnophis sirtalis): a microspectrophotometric, scanning electron microscopic and immunocytochemical study. J. Comp. Physiol. A 181:89.

Simões BF, Sampaio FL, Jared C, Antoniazzi MM, Loew ER, Bowmaker JK, Rodriguez A, Hart NS, Hunt DM, Partridge JC, et al. 2015. Visual system evolution and the nature of the ancestral snake. J. Evol. Biol. 28:1309–1320.

Simões, B. F., Sampaio, F. L., Loew, E. R., Sanders, K. L., Fisher, R. N., Hart, N. S., et al. (2016). Multiple rod-cone and cone-rod photoreceptor transmutations in snakes: evidence from visual opsin gene expression. *Proc. R. Soc. B*, *283* (1823).

Spawls S, Howell K, Drewes RC. 2006. Pocket Guide to the Reptiles and Amphibians of East Africa. London: Christopher Helm Publishers.

Starace F, Lambert V. 2013. Serpents et amphisbènes de Guyane française. Ibis Rouge

Thorpe A. 1991. Spectral trtansmission and short–wave absorbing pigments in the lenses of fish and other animals. City University, London

Underwood, G. 1966. On the visual-cell pattern of a homalopsine snake. *J. Anat. 100*, 571–575.

Underwood G. 1967. A Contribution to the Classification of Snakes. British Museum Natural History Publications

Underwood G. 1970. The Eye. In: Gans C, Parsons TS, editors. Biology of the Reptilia: Morphology B. Vol. 2. New York: Academic Press. pp. 1–97.

Underwood, G., & Kochva, E. (1993). On the affinities of the burrowing asps Atractaspis (Serpentes: Atractaspididae). *Zool. J. Linn. Soc.*, 107: 3–64.

Walls GL. 1942. The Vertebrate Eye and Its Adaptive Radiation. New York: Fafner Publishing Company

Whitaker R, Captain A, Photographer FA, Chaudhuri S. 2004. Snakes of India. Draco Books

Yokoyama S, Radlwimmer FB. 1998. The “five-sites” rule and the evolution of red and green color vision in mammals. Mol. Biol. Evol. 15:560–567.

Yokoyama S, Starmer WT, Takahashi Y, Tada T. 2006. Tertiary structure and spectral tuning of UV and violet pigments in vertebrates. Gene 365:95–103.

Yokoyama S, Tada T, Zhang H, Britt L. 2008. Elucidation of phenotypic adaptations: Molecular analyses of dim-light vision proteins in vertebrates. Proc. Natl. Acad. Sci. USA 105:13480–13485.

Yokoyama S. 2000. Molecular Evolution of Vertebrate Visual Pigments. Prog. Retin. Eye Res. 19:385–419.

Yokoyama S. 2008. Evolution of Dim-Light and Color Vision Pigments. Annu. Rev. Genomics Hum. Genet. 9:259–282.